DIPLOMARBEIT

Titel der Diplomarbeit:

"Cell cycle dependent regulation of the Dam1 kinetochore complex by Cdk1"

Verfasserin:

Veronika Fitz

angestrebter akademischer Grad:

Magistra der Naturwissenschaften (Mag.rer.nat.)

Wien, 2011

Studienkennzahl: A 490
Studienrichtung: Diplomstudium Molekulare Biologie
Betreuer: Dr. Stefan Westermann

Contents

Zusammenfassung

Kinetochore ankern Plus-Enden der Mikrotubuli an die Zentromere und übertragen deren Dynamik in die direkte Bewegung der Chromosomen. Es wurde gezeigt, daß der Hefe-spezifische Dam1-Komplex sowohl strukturelle als auch regulatorische Elemente beinhaltet, die zur Kinetochor-Mikrotubulikontaktfläche in der Bäckerhefe beitragen (Lampert and Westermann, 2011). Mutationen, die die Funktion dieses Komplexes *in vivo* beeinträchtigen, führen zu Chromosomen-Missegregation und zu gravierenden Spindeldefekten (Cheeseman et al., 2001a; Janke et al., 2002). Während die Rolle des Komplexes in Bezug auf das Etablieren von Kinetochore-Mikrotubuliverbindungen ausgiebig erforscht ist, ist es nach wie vor nicht klar wie der Komplex zur Erhaltung der Spindelintegrität beiträgt. Ein Hinweis für den Mechanismus, der diesem Phänotypen unterliegt, kommt von einer neuesten Studie, in der gezeigt wurde, daß Cdc28 (Cdk1)-abhängige Phosphorylierung des Dam1-Komplexes die Dynamik der Mikrotubuli in der Metaphase und Anaphase A beeinflußt (Higuchi and Uhlmann, 2005).

Die Aufreiningung des Dam1-Komplexes aus Hefeextrakten und dessen weiterführende massenspektrometrische Analyse enthüllte weitere Cdk1-Phosphorylierungsstellen. Diese Entdeckung machte es möglich eine übergreifende Studie in Bezug auf die Regulierung des Dam1-Komplexes durch Phosphorylierung sowohl *in vivo* als auch *in vitro* durchzuführen. Zu diesem Zweck wurde eine Serie an rekombinanten Dam1 Phosphomutanten darauf getestet, in wie fern die Haupteigenschaften des Komplexes wie dessen Stabilität, dessen Fähigkeit Ringe auszubilden und dessen Mikrotubulibindungsaffinität durch Phosphorylierung beeinflußt werden. Weiters wurden Hefestämme, in denen die spezifischen Phosphorylierungsstellen mutiert waren, weitgehend untersucht, um deren *in vivo* Effekt zu charakterisieren. Dabei wurde spezielles Augenmerk auf die Veränderungen der Dam1-Komplexlokalisierung als auch der Spindeldynamik gelegt. Diese Untersuchungen weisen darauf hin, daß die Phosphoregulierung des Komplexes Verbindungen, die sich zwischen zwei Dam1-Komplexen befinden, und dadurch die Ringbildung beeinflußt, was sich in einer veränderten Spindeldynamik äußert.

Dieser regulatorische Mechanismus, der der Funktion des Dam1-Komplexes unterliegt, bekräftigt die Vorstellung der Existenz des Dam1-Ringmodels *in vivo*.

Abstract

Kinetochores anchor microtubule (MT) plus-ends at the centromere and translate their dynamics into directed movement of chromosomes during mitosis. The fungal-specific Dam1 complex was previously reported to constitute a major structural and regulatory element of the kinetochore-microtubule interface in budding yeast (Lampert and Westermann, 2011). Mutations that cripple Dam1 function *in vivo* phenotypically result in chromosome mis-segregation and severe spindle defects (Cheeseman et al., 2001a; Janke et al., 2002). While the role of the complex in establishing kinetochore-microtubule attachments has been intensively studied it is less clear how Dam1 directly contributes to maintenance of spindle integrity. A mechanistic hint comes from a previous study that demonstrated that Cdc28 (Cdk1)-dependent phospho-regulation of Dam1 influences microtubule dynamics in metaphase and anaphase A after artificially induced sister-chromatid separation (Higuchi and Uhlmann, 2005).

Purification of the Dam1 complex from yeast extracts and further mass-spec analysis revealed additional Cdk1-sites allowing to conduct a comprehensive study on Dam1 phospho-regulation *in vitro* and *in vivo*. To this end, a series of recombinant Dam1 phospho-mutants have been probed for changes in major Dam1 complex properties such as complex stability, ring formation and microtubule binding affinity. The generation of several Dam1 phospho-mutant yeast strains allowed to characterize the effects *in vivo* by monitoring changes in Dam1 complex localization patterns and measuring altered spindle microtubule dynamics. The data suggest that Cdk1 phospho-regulation influences inter-complex connections and thereby ring formation that influences the dynamics of the mitotic spindle. This regulatory mechanism of Dam1 complex function strengthens the argument for the existence of the Dam1 ring model *in vivo*.

1 Introduction

Cell growth and division are hallmarks of life. The development of new cells requires the division of pre-existing cells. In order to reproduce cells must replicate their genetic material and further segregate it into the two newly formed daughter cells. These cell cycle events have to be tightly regulated in order to fulfill the criteria for successful propagation of life.

The cell cycle of all eukaryotes underlies common principles and key proteins regulating major cell cycle events are conserved from yeast to human. This makes budding yeast, *S. cerevisiae,* a valid model organism to study the cell cycle since it offers many advantages. Besides its general features of short duplication times (90 minutes) and its small, relatively simple and fully sequenced genome it provides very powerful genetic tools to study gene function (Morgan, 2007).

Additionally the more simplified kinetochore architecture of *S. cerevisiae*, which first assembles at point centromeres, the simplest form of centromeric arrangement found in eukaryotes, and second attaches to a single microtubule unlike to multiple in higher eukaryotes, provides a very attractive and simplified model system to visualize kinetochore dynamics and chromosome behavior during cell division (Westermann et al., 2007).

1.1 The budding yeast cell cycle:

The cell cycle consists of continuous events referred to as cell growth and periodic events involving DNA replication and mitosis.

During cell growth most cellular components have to be newly synthesized in order to be passed on to the next generation. The periodic events are generally subdivided into four phases: G1 phase (pre-synthetic gap), S-phase (DNA synthesis), G2 (post-synthetic gap) and M-phase (mitosis), although no G2 phase is described in budding yeast since S-phase was shown to overlap partially with prometaphase, an early mitotic stage (Morgan, 2007; Murray and Hunt, 1993).

1.1.1 Interphase:

To allow progression through the cell cycle, passing the key control point START at the G1-S transition, two requirements have to be fulfilled: enough nutrients have to be provided by the environment and the yeast cell has to reach a certain threshold size. Progression through START promotes cell cycle events like bud emergence, spindle pole body (SPB) duplication and DNA replication. The duplication of the genetic material is a crucial step during cell division. This process is highly regulated ensuring that chromosome replication is completed before the onset of mitosis involving the G2/M checkpoint, which monitors replication fidelity. The two newly formed sister chromatids are held together by a protein complex called cohesin, which consists of four proteins Smc1, Smc3, Scc1 and Scc3 and is thought to topologically entrap sister DNA by forming a ring (Morgan, 2007; Murray and Hunt, 1993).

1.1.2 Mitosis:

Chromosome segregation is a key function during cell division and is referred to as mitosis consisting of four major events in budding yeast: prometaphase, which overlaps partially with S-phase, metaphase, anaphase and telophase.

Yeast undergoes a closed mitosis, in which no nuclear envelope breakdown occurs leaving the nucleus intact throughout the whole cell cycle. The SPB representing the only microtubule-organizing center (MTOC) in yeast, must give rise to both nuclear and cytoplasmic microtubules. Therefore the SPB is embedded in the nuclear envelope facing both sites. Prior to mitotic entry the duplicated SPBs have to be positioned at opposite poles to carry out their function in initiating the formation of a bipolar spindle (kinetochore-MTs and interpolar MTs) as well as the nuclear positioning (astral MTs) (Jaspersen and Winey, 2004). Thereby microtubules emanating from opposite poles attach to kinetochores, huge protein complexes assembled at centromeric regions, by a so-called "search-and-capture" mechanism (Kirschner and Mitchison, 1986), leading eventually to a bi-oriented conformation (amphitelic attachment) of the two sister chromatids in metaphase. This state is intimately monitored by the so-called spindle assembly checkpoint (SAC). An incorrect attachment geometry (syntelic, monotelic, meritelic attachment) results in a loss of tension between the sister chromatids, which can be sensed by Aurora B (Ipl1p in yeast), the catalytic component of the chromosomal passenger complex (CPC). Ipl1 was shown to trigger the turnover of incorrect

attachments by phosphorylating kinetochore components such as the Dam1- and Ndc80-complexes, which are involved in the establishment of MT-kinetochore attachments (Biggins and Murray, 2001; Gestaut et al., 2008; Pinsky et al., 2006; Tanaka et al., 2002). Unattached kinetochores trigger the spindle assembly checkpoint and block progression into anaphase (Lampson and Cheeseman, 2010). However, once the checkpoint has been satisfied a cascade of events leads irreversibly to the separation of the sister chromatids and subsequent exit from mitosis. This involves the activation of a key regulator, the anaphase promoting complex (APC), which together with its activator Cdc20p allows ubiquitination and further degradation of its targets (Thornton et al., 2006; Yoon et al., 2002; Zachariae et al., 1998b). The major functions of the APC at anaphase onset are the proteolysis of mitotic cyclins, a process essential for Cdk1 inactivation and subsequent exit from mitosis, and its role in sister-chromatid separation. The latter involves the degradation of the Separase inhibitor Securin (Pds1p in budding yeast), which leads to cohesin cleavage resulting in two separated DNA molecules (Morgan, 2007; Peters, 2006; Peters et al., 2008). Chromosome segregation is achieved by the contribution of two mechanisms, the pulling of the sister chromatids to opposite poles by depolymerizing microtubule plus ends (anaphase A) and the elongation of the distance between the two poles (anaphase B). In budding yeast anaphase A and anaphase B are overlapping events. In addition the astral microtubules are also thought to play an important role in chromosome segregation by correctly positioning the mitotic spindle (Straight et al., 1997). Telophase, which is defined by spindle disassembly, is followed by cytokinesis, the final step in cell division. The budding off of the new daughter cell is executed by the action of a contractile ring after successful segregation of the daughter nucleus into the bud (Balasubramanian et al., 2004; Morgan, 2007; Tanaka et al., 2005).

1.2 Cell cycle regulation in budding yeast:

The cyclin dependent kinases (Cdks) are the "drivers" of the eukaryotic cell cycle. They are absolutely required to coordinate all cell cycle events in a timely manner. Cdc28p is the major cell cycle kinase in budding yeast. The timing and specificity of its action depend on the association with its activating subunits, the so-called cyclins. Mechanisms like the differential transcription of cyclins themselves, their degradation, the association of cyclin-Cdk complexes with Cdk-inhibitors and posttranslational modifications of Cdks contribute to the specificity of cyclins throughout the cell cycle (Bloom and Cross, 2007; Morgan, 1997, 2007; Murray and Hunt, 1993). Recent studies have revealed hundreds of Cdk1-substrates involving factors regulating Cdk1 function itself or other proteins required in DNA replication or spindle assembly (Holt et al., 2009; Ubersax et al., 2003). This reflects the global regulatory strategy, by which Cdk1 phosphorylation coordinates a variety of different cell cycle events (Holt et al., 2009; Ubersax et al., 2003).

The irreversible switch at the START point towards cell cycle engagement involves the action of Cdk1. Once the cell has reached a critical size the accumulated G1 cyclin Cln3 associates with Cdc28p leading to the initiation of transcription of the G1 cyclins Cln1 and 2 (Dirick et al., 1995; Stuart and Wittenberg, 1995; Tyers et al., 1993) and the S-phase cyclins Clb5 and 6 (Schwob and Nasmyth, 1993) through activation of the transcription factors SBF and MBF. High levels of G1-cyclins then lead to the inactivation of the anaphase promoting complex APC, which targets S- and M-cyclins for their destruction, via phosphorylation of Cdh1 allowing respective cyclins to accumulate (Jaspersen et al., 1999; Kotani et al., 1999; Kramer et al., 2000; Zachariae et al., 1998a). In addition, the degradation of Sic1p, which inhibits Clb5/6-Cdc28, is triggered by G1 cyclins leading to S-phase transition (Mendenhall and Hodge, 1998). Progression through START promotes cell cycle events like bud emergence, spindle pole body (SPB) duplication and DNA replication, events that were shown to be tightly regulated by Cdk1 function. At the end of S phase the transcription of mitotic cyclins (Clb1-4) is switched on. Their accumulation directs repression of the transcription of SBF-dependent G1-cyclins, maintenance of Sic1-destruction and additionally their own expression. The mitotic Clb-Cdc28 complexes are negatively regulated by Swe1 phosphorylation, a mechanism, which controls the timing of mitotic entry by mediating mitotic delay in response

to decreased bud size (morphogenesis checkpoint). Dephosphorylation of Clb-Cdc28 by Cdc25p then drives mitotic progression (Bloom and Cross, 2007; Morgan, 1997).

The mitotic cyclins Clb1-4 drive spindle assembly, correct spindle positioning and were shown to contribute to the movement of the nucleus into the bud neck and to control chromosome segregation (Chee and Haase, 2010; Richardson et al., 1992; Schwob and Nasmyth, 1993). Clb-Cdc28 is further involved in regulating indirectly microtubule-kinetochore attachments by phosphorylating the passenger complex components Bir1p and Sli15p and thereby keeping Ipl1p at the kinetochore where it is believed to act as main tension-sensor (Bouck and Bloom, 2005; Enserink and Kolodner, 2010; Widlund et al., 2006). Once the spindle assembly checkpoint has been satisfied metaphase-to-anaphase transition is triggered by ubiquitination of Pds1 by the APC, resulting in its proteasomal degradation and the liberation of Separase (Esp1 in budding yeast), which then cleaves the Scc1p-subunit of the cohesin complex that holds the two sister chromatids together. Two mechanisms contribute to efficient downregulation of Cdk1 activity, a state considered to be crucial for further cell cycle progression: the destruction of mitotic cyclins by the APC and the release of Cdc14p from the nucleolus, the main phosphatase reversing Cdk1 phosphorylation (Bloom and Cross, 2007; Enserink and Kolodner, 2010; Morgan, 1997; Queralt and Uhlmann, 2008).

The combination of cohesion resolution and downregulation of Cdk1 has been recently reported to be sufficient to allow proper chromosome segregation (Oliveira et al., 2010).

At the end of mitosis Cdc14p dephosphorylates Cdh1 to allow its re-association with the APC leading to further destruction of mitotic cyclins completing the cell cycle. In addition expression of the Cdk1 inhibitor Sic1 at the M-G1 boundary then supports the maintenance of low Cdk1 activity throughout the next G1 phase (Figure 1) (Bloom and Cross, 2007; Enserink and Kolodner, 2010; Morgan, 1997).
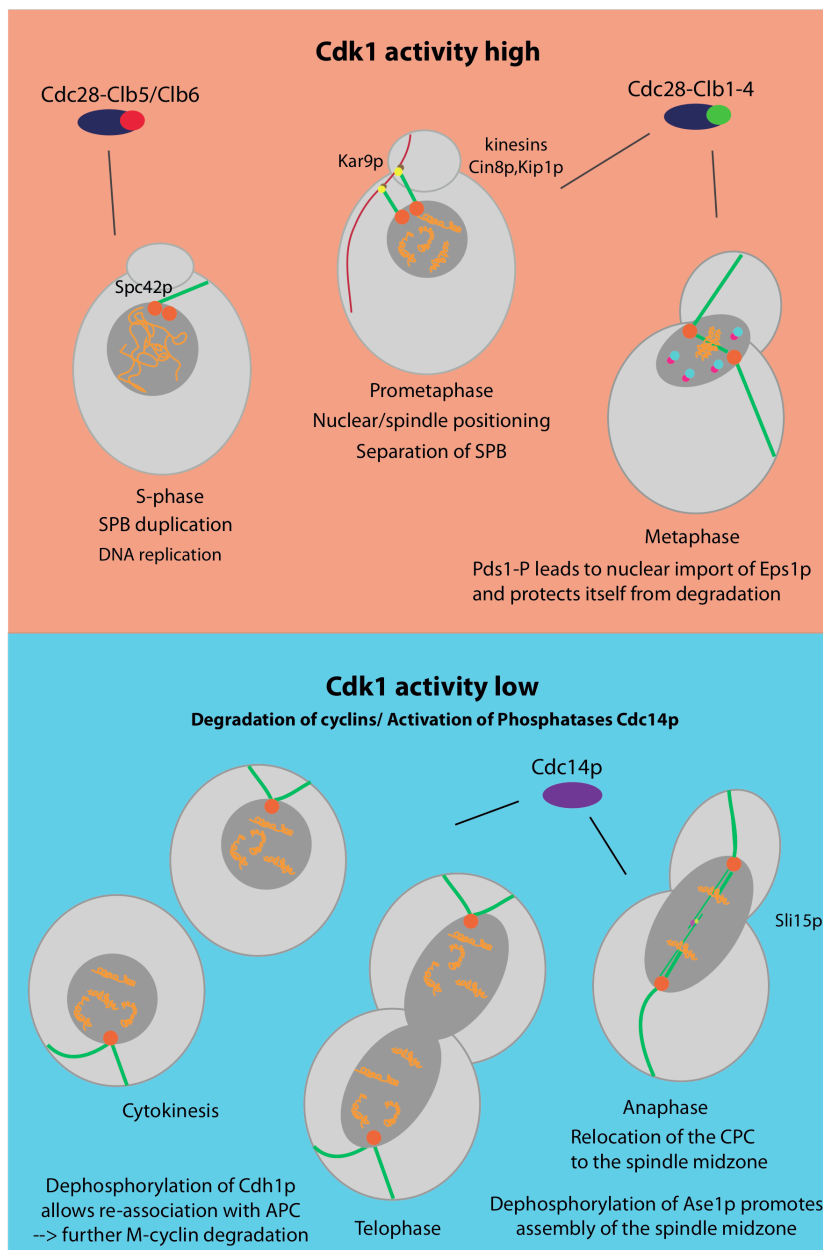
Figure 1: Cell cycle dependent regulation of Cdk1 substrates: Cdk1 is involved in many different cell cycle events as depicted here in this figure. It has main functions in coordinating DNA replication by for example phosphorylating Cdc6 and thereby preventing re-activation of replication origins (Mimura et al., 2004); it also regulates SPB duplication via phosphorylation of Spc42p in S-phase (Jaspersen et al., 2004).

Further during early mitosis its activity is required for positioning the nucleus and the spindle, a process shown to depend on Kar9 phosphorylation (Liakopoulos et al., 2003). Furthermore the separation of the SPB was achieved by phosphorylating kinesin-5 (Chee and Haase, 2010). Phosphoryating Pds1p regulates sister chromatid cohesion by the two mechanisms mentioned in the figure (Agarwal and Cohen-Fix, 2002; Jensen et al., 2001). After anaphase onset Cdk1 action has to be reversed, which contributes to spindle elongation and spindle integrity resulting in efficient chromosome segregation, partially due to dephosphorylation of Sli15 leading to the relocation of the CPC to the spindle midzone (Bouck and Bloom, 2005; Widlund et al., 2006).

1.3 The budding yeast kinetochore:

During cell division the two sister chromatids have to be equally transmitted to the two emerging daughter cells in order to prevent genomic imbalances that could have dramatic effects on viability. One of the requirements to allow faithful chromosome segregation is the correct coupling between the genetic material and the mitotic spindle. The kinetochore, a highly organized protein network, assembles at centromeric DNA and provides the connection to the plus ends of kinetochore microtubules (kMTs). Keeping these attachments stable despite the highly dynamic behavior of microtubules is a challenging task and requires an elaborate control system (Westermann et al., 2007).

The overall organization of the kinetochore is conserved from yeast to human but differs in terms of complexity between different species (Lampert and Westermann, 2011; Santaguida and Musacchio, 2009). Budding yeast displays the simplest kinetochore, binding a single microtubule, whereas the more extensive kinetochore in higher eukaryotes attaches to multiple kinetochore fibres (Santaguida and Musacchio, 2009; Westermann et al., 2007). Conservation of kinetochore components leads to the assumption of a "repeat subunit" model that implies the repetition of the basic MT-binding module of budding yeast in higher eukaryotes (Joglekar et al., 2006; McAinsh et al., 2003; Santaguida and Musacchio, 2009; Westermann et al., 2007; Zinkowski et al., 1991).

1.3.1 Structure of the budding yeast kinetochore:

The organization of the kinetochore shows a highly conserved structure, consisting of three main substructures. The inner layer consists of proteins contacting the centromeric platform. The middle layer constituents function as bridge between inner and outer kinetochore plate, whereas the components of the outer layer provide a direct link to the plus end of microtubules (Figure 2) (Santaguida and Musacchio, 2009; Westermann et al., 2007).
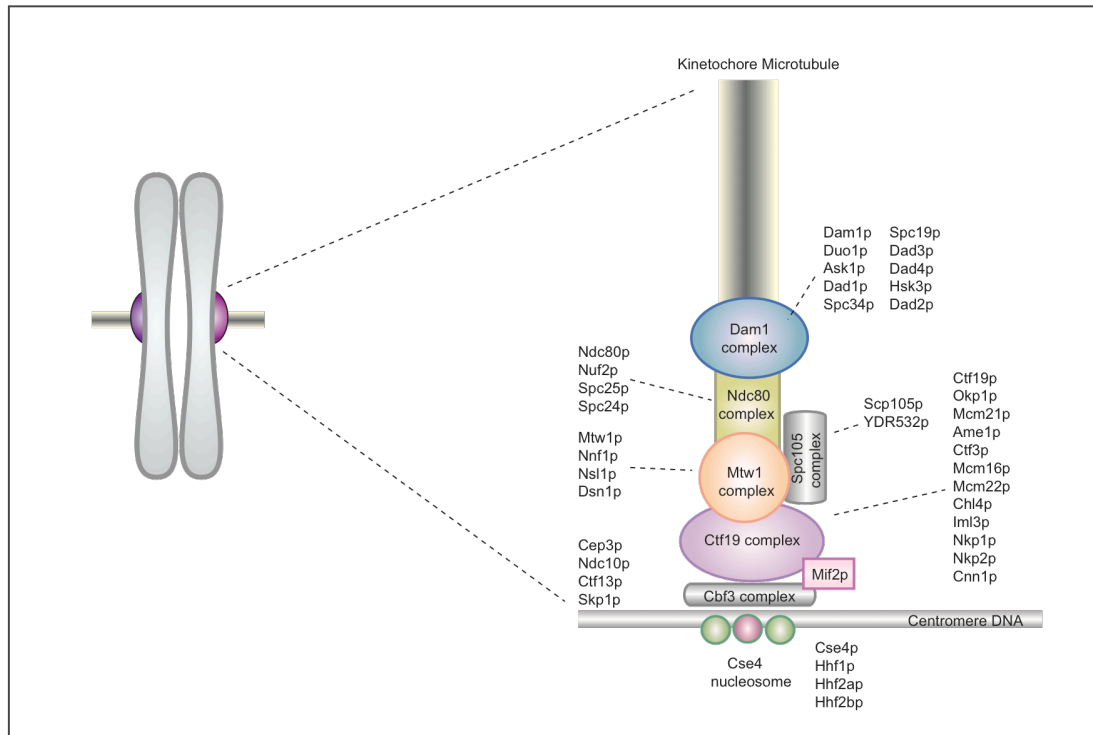
Figure 2: Organization of the budding yeast kinetochore (adapted from Lampert and Westermann, 2011)

1.3.2 Centromeric organization:

The centromeric region present on each chromosome in budding yeast is referred to as a "point centromere" consisting of only 125 bps and divided into three conserved elements termed the centromere defining elements CDE I, CDE II and CDE III (Fitzgerald-Hayes et al., 1982). These elements are characterized by two short DNA regions, namely CDE I (8bps) and CDE III (25bps), separated by a 78- to 86- bps A+T-rich CDE II (>90% A+T) element (Hegemann and Fleig, 1993). This sequence-delimited DNA stretch was shown being wrapped around a single specialized nucleosome containing the histone H3 variant CENP-A (Cse4p in *S. cerevisiae*) (Keith and Fitzgerald-Hayes, 2000; Meluh et al., 1998). This centromeric organization was shown to be absolutely required and sufficient to drive proper kinetochore assembly (Goshima and Yanagida, 2000; Meluh et al., 1998). The fungal CBF3 complex, made up of four essential proteins - Ndc10p, Ctf13p, Cep3p, and Skp1p, binds to the CDE III element in a sequence-specific manner (Espelin et al., 1997; Lechner and Carbon, 1991), exhibiting the primary step in a subsequent cascade of assembling events (McAinsh et al., 2003; Santaguida and Musacchio, 2009; Westermann et al., 2007).

1.3.3 The inner kinetochore plate:

The interlinkage between the centromere and the kinetochore in budding yeast is made up by the Ctf19 complex (De Wulf et al., 2003), providing direct contact to the centromeric region, involving the probably direct interaction of Mif2p with the Cse4 nucleosome (Meluh and Koshland, 1995). The Ctf19 complex, which is referred to as the CCAN network in humans, consists of about 13 proteins building up at least one stable subcomplex, the COMA complex (Ctf19p, Okp1p, Mcm21p and Ame1p) (De Wulf et al., 2003). It has been shown that only Okp1p and Ame1p are essential in budding yeast and that all other members of the Ctf19 complex are dispensable for viability although their loss results in increased chromosome missegregation (Ghosh et al., 2001). This feature is unique to the Ctf19 complex since all other kinetochore components seem to be absolutely required for viability (Santaguida and Musacchio, 2009; Westermann et al., 2007).

1.3.4 The bridge between inner and outer layer:

Three complexes are involved in building up the so-called KMN (KNL-1 MIS12 NDC80) network: the Spc105 complex, the Mtw1 complex and the Ndc80 complex (Cheeseman et al., 2006; Nekrasov et al., 2003). The Spc105 complex constitutes of Spc105p and Kre28p that associate in a 1:2 stoichiometry in order to form a heterotrimeric complex (Pagliuca et al., 2009). The recruitment of the Spc105 complex to centromeric DNA was shown to depend on CBF3 complex (De Wulf et al., 2003; Pagliuca et al., 2009). There is also evidence that this highly elongated complex spans the whole kinetochore structure binding weakly to microtubules. However the Spc105 complex is not required for the establishment of MT attachments per se but was shown to be involved in ensuring bi-orientation of sister chromatids on the mitotic spindle (Pagliuca et al., 2009).

The conserved Mtw1 complex forms a heterotetramer assembled from two stable heterodimers Mtw1p - Nnf1p and Dsn1p - Nsl1p (Euskirchen, 2002; Hornung et al., 2010). This complex displays direct interaction with the microtubule-binding Ndc80 complex (Hornung et al., 2010). Mutations in this complex that cripple its function result in bi-orientation and chromosome segregation defects (Cheeseman et al., 2004). Recent biochemical interaction studies shed light on the arrangement of this complex within the

kinetochore context where the Mtw1p – Nnf1p subcomplex is rather oriented towards the inner platform, speculated to interact with the COMA subcomplex of the Ctf19 complex, whereas the Dsn1p – Nsl1p dimer is interacting with the Spc24p/Spc25p heterodimer of the Ndc80 complex (Hornung et al., 2010).

The central component of the kinetochore – microtubule interface in all eukaryotes is the so-called Ndc80 complex, a complex consisting of four essential proteins Spc24p, Spc25p, Nuf2p and Ndc80p that are responsible for direct interaction between the kinetochore structure and the microtubule lattice (Janke et al., 2001; Wigge and Kilmartin, 2001). Thereby the Spc24p/Spc25p heterodimer forms a globular head domain and was shown to mediate the connection towards the Mtw1 subcomplex Dsn1p – Nsl1p, as mentioned above. On the other side the Nuf2p – Ndc80p heteodimer forms a long coiled-coiled region with an N terminal head domain (Alushin et al., 2010). Within this N terminal region resides the MT-binding capacity of the Ndc80 complex, which more precisely is restricted to the presence of two interacting calponin homology (CH) domains (Wei et al., 2007). The Ndc80p CH domain was shown to bind highly conserved binding sites within the microtubule lattice, the intra-dimer and inter-dimer microtubule interfaces, whereas the Nuf2p CH domain interacts electrostatically with the negatively charged, flexible C terminus of tubulin, referred to as E-hook (Alushin et al., 2010). The Ndc80 complex is absolutely required for the recruitment of further outer kinetochore components such as the microtubule-binding Dam1 kinetochore complex and Stu2p, a microtubule-associated protein (MAP) of the XMAP215 family regulating spindle dynamics during spindle orientation and metaphase chromosome alignment (He et al., 2001). Although the Ndc80 complex is essential to allow proper formation of kinetochore-microtubule attachments, alone it is not sufficient to drive chromosome segregation in budding yeast (Janke et al., 2001; Wigge and Kilmartin, 2001). The Ndc80 complex cooperates with the fungal specific Dam1 complex *in vivo* in order to maintain stable microtubule-kinetochore attachments allowing proper sister chromatid separation (Lampert et al., 2010; Lampert and Westermann, 2011; Tien et al., 2010; Westermann et al., 2007).

1.3.5 The microtubule – kinetochore interface:

The coupling of chromosome movement to the microtubule depolymerization during anaphase A was shown to depend on the Dam1 complex that constitutes of 10 subunits:

Dam1p, Ask1p, Spc34p, Spc19p, Duo1p, Dad1p, Dad2p, Dad3p, Dad4p and Hsk3p (Cheeseman et al., 2001a; Cheeseman et al., 2001b; Enquist-Newman et al., 2001; Hofmann et al., 1998; Janke et al., 2002; Jones et al., 1999). Dam1 complex mutants display two different phenotypes - loss in spindle integrity as well as high rates of chromosome missegregation. In addition a subclass of mutants show metaphase arrest because of attachment defects resulting in the activation of the spindle assembly checkpoint (Cheeseman et al., 2001a; Janke et al., 2002). Its localization is not restricted to the outer kinetochore but also exhibits a continuous decoration along spindle microtubules (Jones et al., 2001). The heterodecameric Dam1 complex was shown to bind microtubules *in vitro* and form different geometric configurations along the microtubule lattice – either small oligomeric patches or a ring-like structure assembling around microtubules *in vitro* (Figure 3) (Cheeseman et al., 2001a; Miranda et al., 2005; Westermann et al., 2005). The Dam1 complex was shown to act as autonomous and continuous plus-end tracker *in vitro* and to stabilize GDP-bound microtubules (Grishchuk et al., 2008; Lampert et al., 2010; Tien et al., 2010; Westermann et al., 2005). The ring model suggests a beautiful mechanism for coupling microtubule disassembly to chromosome movement, where the peeling off of protofilaments pushes the ring towards the opposite spindle poles. Thereby it would act as a force coupler, translating the energy released from microtubule disassembly into chromosome movement (Grishchuk et al., 2008; Westermann et al., 2006). Nevertheless, so far the existence of a Dam1 ring could not be shown *in vivo*.
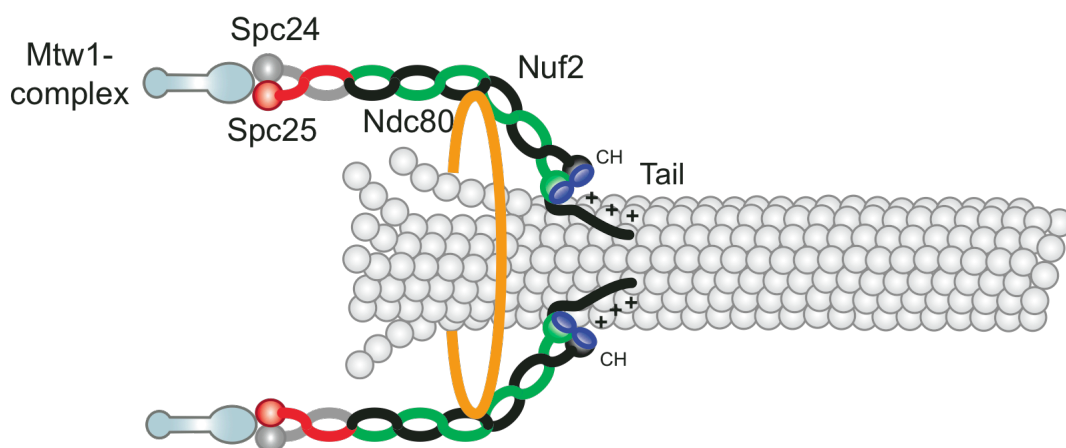
Figure 3: Model of the ring-like structure of the Dam1 complex: The Dam1 complex assembles around microtubules in either oligomeric patches or into rings (adapted from Lampert and Westermann, 2011)

Assembly of the 16–fold Dam1 ring complex was assumed to be engaged by the connection with an arriving spindle microtubule initiating a large conformational change in the complex (Wang et al., 2007). Recent data argument against the assumption that large conformational changes must occur upon oligomerization around microtubules and that the Dam1 ring complex arranges into a 15-fold symmetry around the 13-protofilament microtubules including two interfaces between two adjacent complexes required for this oligomerization mechanism (Ramey et al.). The proteins that are believed to be involved in these interactions are the C-terminus of Dam1p together with Spc34p and the C-terminus of Ask1p together with a not yet assigned component of the complex; partner candidates for this second interaction are Duo1p, Dam1p, Dad1p, Dad3p, Spc34p or Spc19p (Figure 4) (Ramey et al., 2011).
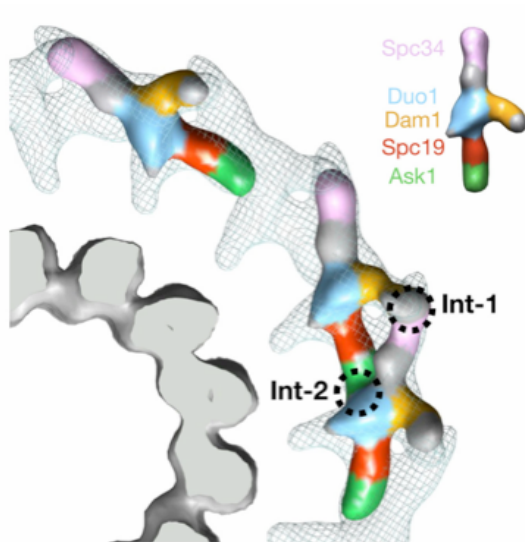
Figure 4: Modeling of individual Dam1 complexes into the ring-like structure around microtubules: The microtublule structure is depicted here as solid gray structure, whereas the Dam1 ring structure is shown in a mesh-like appearance. The structure of single Dam1 complexes derived from negative stain EM analysis reflects the location of single components within the complex itselft, as well as the dimer conformation with the two indicated interfaces (adapted from Ramey et *al*., 2011)

The C-terminus of the Dam1p subunit (three out of four phospho-sites: S257A S265A S292A) as well as Spc34p (T199A) are targets of the Ipl1 kinase in order to dissolve incorrect attachments that were not under tension allowing reformation of new microtubule-kinetochore attachments (Cheeseman et al., 2002). Phosphorylation of Dam1p was shown not to affect its binding affinity to microtubules per se but its ability to form rings (Westermann et al., 2005).

The C-terminus of Ask1p gets phosphorylated by Cdk1p in a cell cycle dependent manner including S216 and S250 (Li and Elledge, 2003). Ask1p dephosphorylation results in stabilization of the anaphase spindle, increasing chromosome segregation fidelity under conditions where anaphase has been artificially induced upon cohesin cleavage (Higuchi and Uhlmann, 2005). This leads to the assumption that posttranslational modification of these subunits may regulate their function *in vivo* by regulating their assembly state. The connection between the Dam1 complex and the central kinetochore is mediated by Dam1p and Ndc80p of the Ndc80 complex. This interaction is also regulated by Ipl1 phosphorylation in order to establish biorientation (Lampert et al., 2010; Tien et al., 2010). Recent data suggest that the microtubule-binding interface is made up by the N-terminal region of Dam1p and Duo1p, a model that contradicts earlier observations done by Wang et *al*., where the C-terminal domain of Dam1p seemed to protrude towards the microtubule lattice (Ramey et al., 2011; Wang et al., 2007).

1.4   Aim of the project

An essential function of the kinetochore is the coupling of chromosome movement to microtubule depolymerization, allowing proper segregation of the genetic material to the two daughter cells. In order to do so two main requirements have to be fulfilled: Firstly stable attachments between the kinetochore and the spindle microtubules emanating from opposite poles have to be established. Secondly, after cohesin cleavage, which results in the separation of the two sister chromatids, spindle microtubule elongation is initially regulated by suppression of the dynamic instability of microtubules. Mutations that cripple Dam1 function *in vivo* phenotypically result in chromosome mis-segregation and severe spindle defects. While the role of the Dam1 complex in establishing kinetochore-microtubule attachments has been intensively studied it is less clear how Dam1 directly contributes to maintenance of spindle integrity (Cheeseman et al., 2002; Cheeseman et al., 2001a; Janke et al., 2002). A mechanistic hint comes from a previous study that demonstrated that dephosphorylation of Cdc28 (Cdk1)-phospho-sites within Ask1p, a Dam1 complex subunit, decreases microtubule dynamics in metaphase as well as in anaphase after artificial cleavage of cohesin, leading to improved chromosome segregation fidelity (Higuchi and Uhlmann, 2005). This reflects the

assumption that resolution of cohesion and downregulation of Cdk1 are sufficient to allow proper chromosome segregation (Oliveira et al., 2010). With the aim to decipher the regulatory role for Cdk1 phosphorylation of the Dam1 complex in mitotic spindle function it is crucial to identify all potential Cdk1 phospho-sites within this complex. Further investigation of changes in Dam1 complex properties, such as MT binding activity or ring formation, according to the phosphorylation state was done by performing a detailed biochemical analysis of different Dam1 phospho-mutants. In order to decipher functional consequences *in vivo* I used life cell microscopy of yeast strains harboring mutations within the Cdk1 phospho-sites of the Dam1 complex.

2 Results:

2.1 Identification of a novel Cdk1 substrate within the Dam1 complex

A previous study on Dam1 complex phospho-regulation identified two sites in the Ask1 subunit that are targeted by the cell cycle kinase Cdk1 *in vivo*. Ask1p phosphorylation is timely regulated peaking at metaphase and decreasing after anaphase onset (Li and Elledge, 2003). However, it was reported that both phospho-mimicking and non-phosphorylatable mutants of Ask1p did not show an obvious growth phenotype. Interestingly in the context of a temperature sensitive *ask1-3* mutant background the Ask1 phospho-null mutants failed to grow at the permissive temperature. This suggests that Cdk1 phosphorylation might have a positive effect on Ask1 activity (Li and Elledge, 2003). To understand the function that underlies Dam1 complex regulation I screened for potential additional Cdk1 phospho-sites.

2.1.1 Mapping of a novel Cdk1 phospho-site within the Dam1 complex *in vivo*:

To this end I performed two-step purifications from unsynchronized yeast cultures, where the Dad1p subunit of the complex was fused to a S-tag-TEV-ZZ modified TAP tag at its C-terminus. Purified proteins were detected by silver staining (Figure 5). The elution, giving the highest yield, was chosen for further mass spec analysis to identify potential phospho-sites within these proteins. Three independent experiments were performed. For Ask1 we could confirm the phospho-site at position S216. However the phospho-site at position S250 could not be detected *in vivo*. This is possibly due to a low sequence coverage of the protein of interest. Interestingly Spc19p, a small protein (165 aa) of about 19 kDa, was shown to be modified at position S116, overlapping with a Cdk1 minimal consensus site (SP).
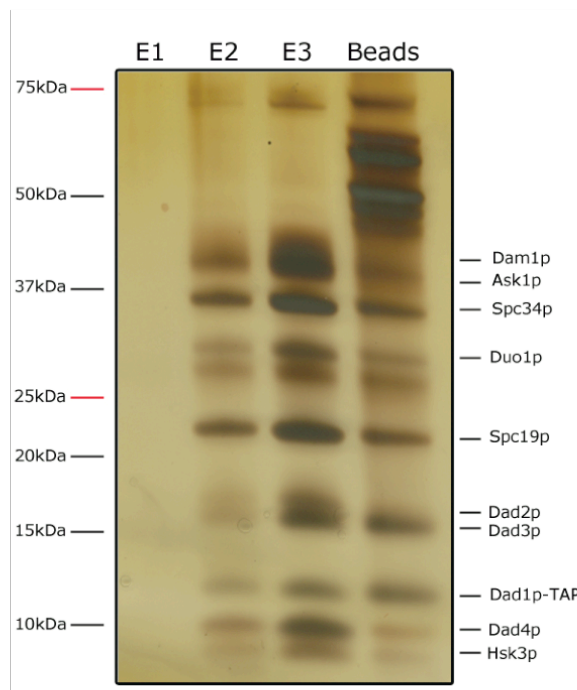
	1st purification	2nd purification	3rd purification
Ask1 S216		+	+
Ask1 S250			
Spc19 S116	+	+	+

Figure 5: Silver gel of TAP-tag purified Dam1 complex: All ten subunits were detected on the gel. Elution E3 was subjected for further MS analysis.

2.1.2 Confirmation of Spc19p as a novel Cdk1 substrate by *in vitro* phosphorylation

To confirm Spc19p as new Cdk1 substrate an *in vitro* kinase assay was performed. To this end recombinant WT Dam1 complex purified from bacteria (Miranda et al., 2005; Westermann et al., 2005) was incubated with TAP tag purified Clb2-Cdc28 in presence of either cold ATP or hot γ-[^{32}P] ATP. The latter condition allowed to determine the saturation of substrate phosphorylation by the kinase over time. The time course experiment revealed that saturation was reached after 30 minutes for Ask1p. At this time point (T30) both phospho-sites S216 and S250 were detected by MS analysis. Although a signal for Spc19p phosphorylation was not detected by autoradiography the phospho-peptide could be assigned by MS analysis after one hour (Figure 6).

	after 30'	after 60'
Ask1 S216	+	+
Ask1 S250	+	+
Spc19 S116		+
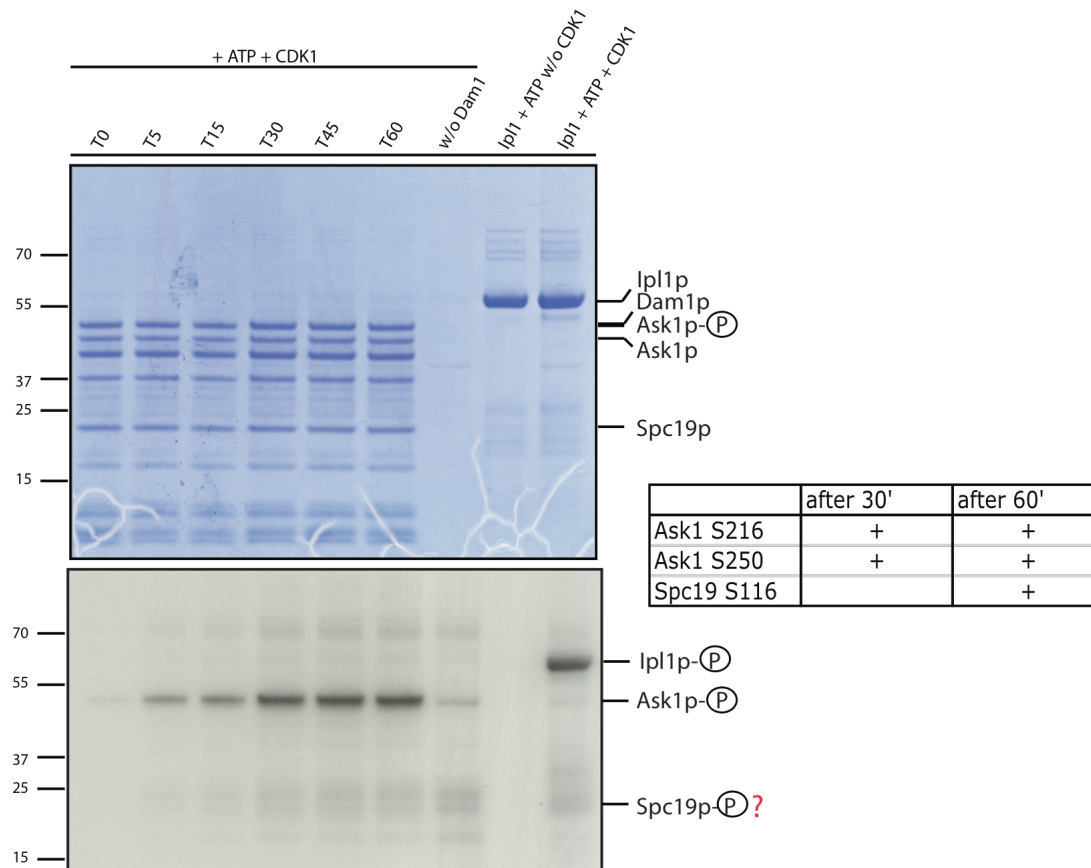
Figure 6: Time course of Dam1 *in vitro* phosphorylation: Phosphorylation of Ask1p is saturated after 30 minutes. The signal for the phosphorylated Ask1p species migrates together with Dam1p in the gradient gel (4-12%). Phosphorylation signal for Spc19p is not detectable by radioautography throughout the whole time course. Identification of phospho-sites at two different time points by MS analysis indicated in the box. Ipl1p was used as control.

After mapping a novel Cdk1 dependent phosphorylation of Spc19p both *in vivo* and *in vitro* I wanted to further examine Spc19p phosphorylation *in vivo.* Therefore I investigated whether a faster migrating species, indicative for a phosphorylation modification, was detectable for Spc19p by WB. Similar experiments have been previously performed for the phospho-protein Ask1p (Li and Elledge, 2003). With the aim to enrich for the protein I immunoprecipitated Spc19-3xHA from asynchronous yeast cultures either in presence or absence of phosphatase inhibitors. The phosphatase inhibitor-free sample was then subsequently treated with λ-phosphatase in order to obtain the faster migrating dephosphorylated species. Both samples were analyzed in parallel by WB demonstrating two differently migrating Spc19 species. Indeed Spc19p was previously suggested to be a phosphoylated protein. This was shown by TAP-tag purification of the Dam1 complex and consecutive phosphatase treatment (Figure 7B, (Cheeseman et al., 2001a)). I could reconstitute the slight difference in migration behavior between the two conditions depicted in Figure 7A.
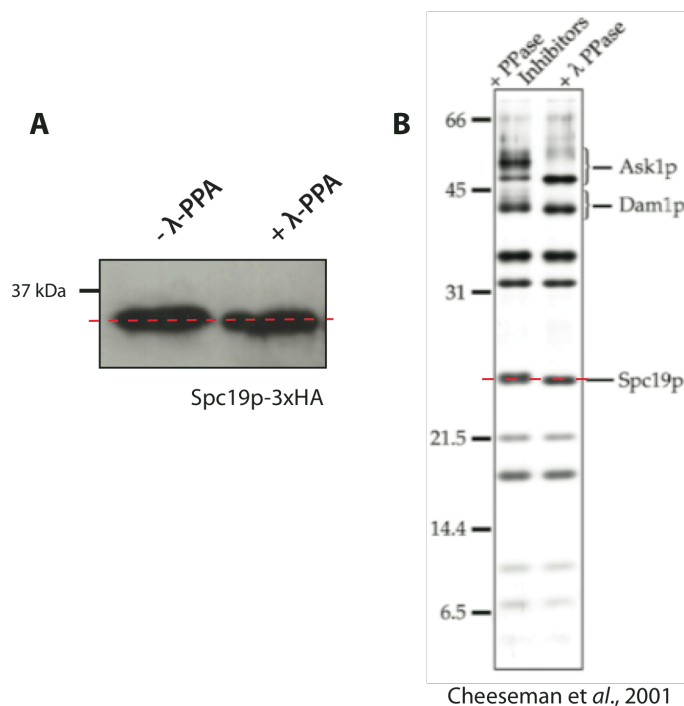
Figure 7: Phospho-shift of Spc19: Figure A illustrates a WB representing immunoprecipitated Spc19-3xHA, where the first sample was treated with phosphatase inhibitors and the second was treated with λ-phosphatase resulting in two slightly differently migrating species. Figure B shows the same result for TAP-tag purified Spc19p after incubation with either phosphatase inhibitors or λ-phosphatase (Cheeseman et al., 2001a).

In summary, I could confirm that S216/S250 within Ask1p are targeted by Cdk1 *in vitro*. However, *in vivo* only S216 could be mapped by MS analysis probably due to low sequence coverage of the protein. Furthermore I was able to reproduce previous results showing that Spc19p is phosphorylated *in vivo* and identify it as a potential novel Cdk1 substrate (Figure 8).
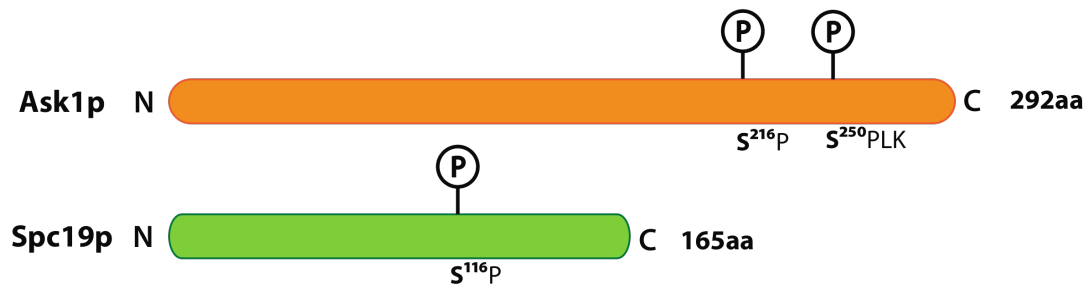
Figure 8: Schematic illustration of Ask1p and Spc19p: Phospho-sites within each protein depicted as P. Only Ask1 S250 exhibits the full Cdk1 consensus site (SPLK), the other two sites contain the minimal consensus site (SP).

2.2 Biochemical characterization of Dam1 complex phospho-mutants

The Dam1 complex has been intensively studied *in vitro*. It was shown to have an intrinsic microtubule binding activity and to oligomerize into rings encircling microtubules, a cooperative process that depends on its concentration (Cheeseman et al., 2001a; Miranda et al., 2005; Westermann et al., 2005). It is conceivable that these parameters are subjected to regulatory inputs. Consequently I wanted to probe how Cdk1 activity influences Dam1 complex integrity, ring formation efficiency and microtubule-binding affinity.

2.2.1 Generation of Dam1 complex phospho-mutants

The first step for a comprehensive biochemical analysis was to generate several Dam1 phospho-mutants, either by using alanine-substitution mutants lacking Cdk1 phosphorylation sites or by using phospho-mimicking mutants, where serines were replaced by glutamic acids. I created Ask1p double mutants as well as triple mutants additionally harboring the mutated Spc19-phospho-site. All mutants were recombinantly expressed in bacteria and purified as previously described by Westermann et *al.* (2005). During initial purification attempts it became apparent that the handling of the alanine-mutants was somewhat more difficult. The complex was relatively unstable and showed an aggregation tendency during dialysis. Probably the instability was a result of amino acid replacement, since the recombinant WT complex purified from bacteria is also in the non-phosphorylated state. Purified Dam1 phospho-mutants are illustrated in Figure 9.
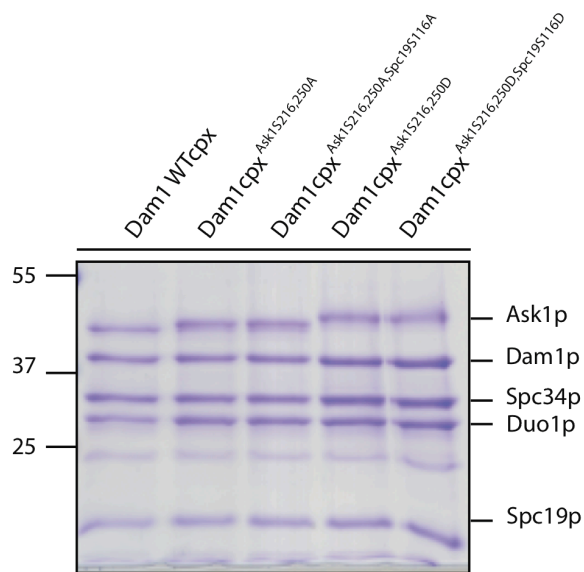
Figure 9: Purification of Dam1 complex (cpx) phospho-mutants: All double and triple mutants could be expressed and purified from bacteria. Both phospho-null and phospho-mimicking mutants of Ask1 appear as slower migrating species.

2.2.2 Phosphorylation of Ask1p is abolished in Ask1-phospho-mutants

To determine whether elimination of the two phospho-sites in Ask1p is sufficient to completely abolish *in vitro* phosphorylation by Cdk1 I again performed an *in vitro* kinase assay using the same conditions as described above at one hour of incubation. The Ask1p specific phosphorylation signal was completely abrogated in all mutants. Therefore we consider these mutants a good tool for simulating the either non-phosphorylated or phosphorylated state of the protein *in vitro*. We couldn't assess Spc19 phosphorylation in these assays since the signal is not detectable in autoradiography as previously shown in section 3.1.3 (Figure 10).
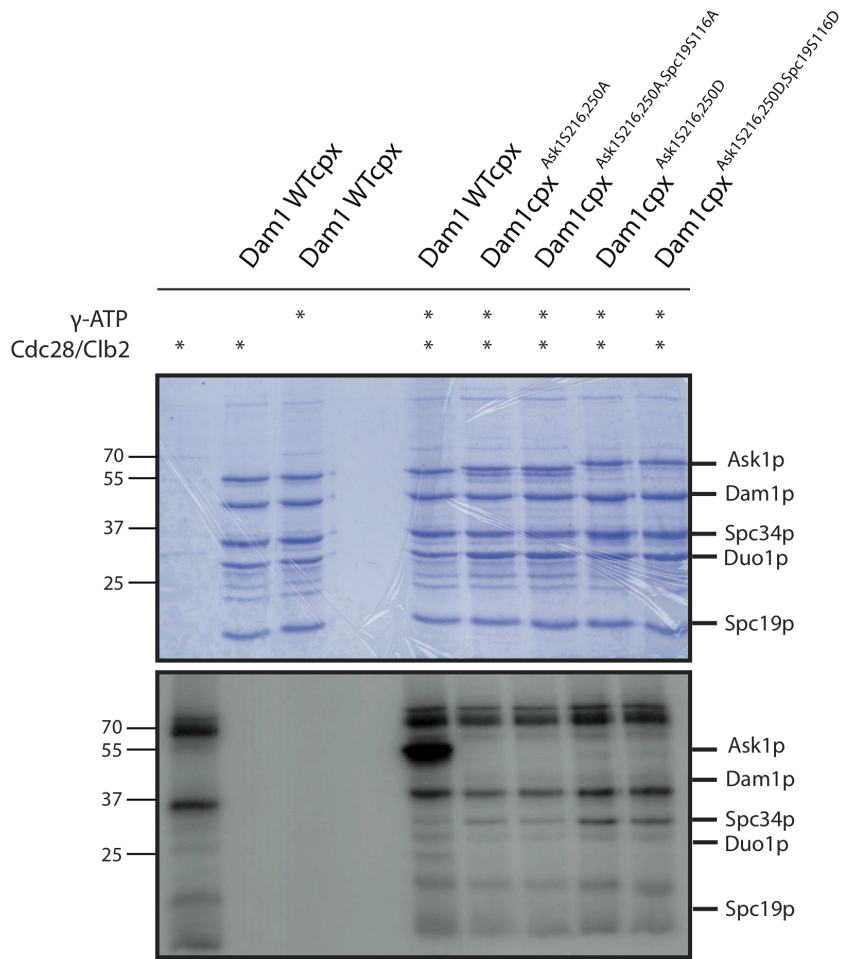
Figure 10: *In vitro* **kinase assay of double/triple phospho-mutants:** Phosphorylation of Ask1 phospho-mutants is completely abolished suggesting that these two sites (S216, S250) are the only Cdk1 phospho-sites within Ask1p. Spc19p did not give any specific phosphorylation signal in the radioautography.

2.2.3 Cdk1 phospho-mutants display similar complex composition as wild type complex

Phosphorylation of proteins is an important cellular switch that can control the on-or-off state of a protein, introduce a conformational change or either interfere or promote protein-protein interactions. To investigate whether phosphorylation of the Dam1 complex has an impact on the overall integrity of the complex I performed size exclusion chromatography. Therefore I used the triple mutants only. The complex integrity for both mutants, phospho-null and phospho-mimicking, was retained during gel filtration. Both mutant complexes elute at the same position as the WT complex indicating an equal stoichiometric composition of Dam1 complex components (Figure 11). Therefore we can assume that Cdk1 activity does not interfere with intra-complex interactions.
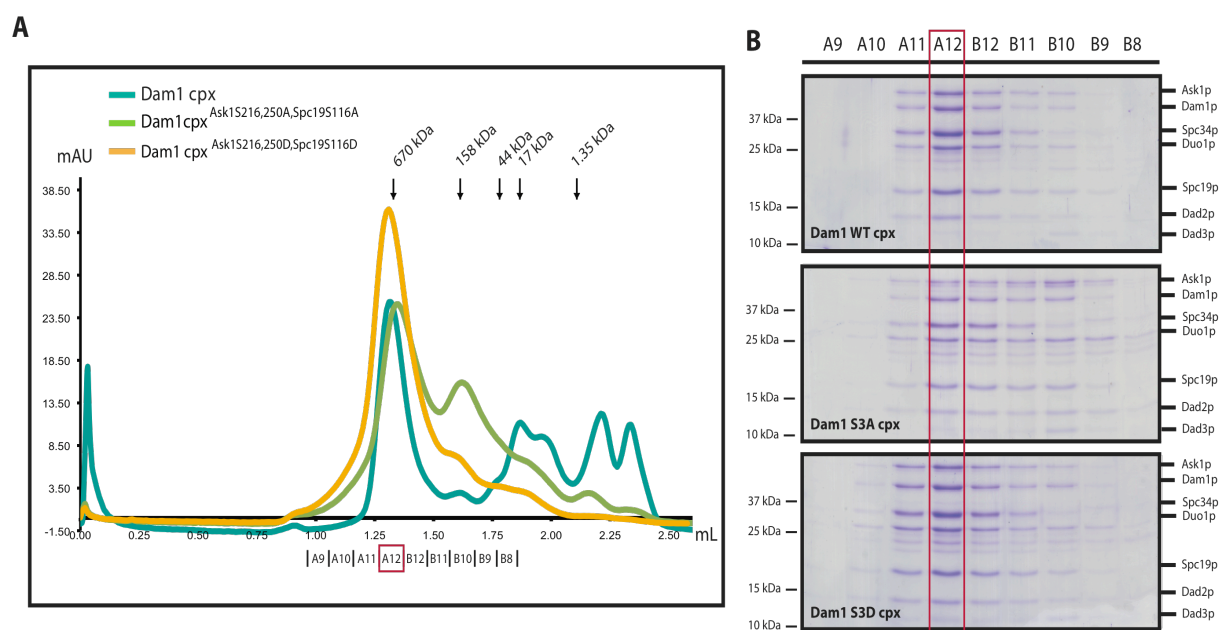
Figure 11: Size Exclusion Chromatography: Complex integrity of Dam1 phospho-mutants was retained during gel filtration. Mutants show equal stoichiometry as WT Dam1 complex. The red boxes in the chromatogram (A) and in the corresponding gels (B) indicate the peak fraction.

2.2.4 Cdk1 regulation has mild effects on microtubule binding activity of the Dam1 complex

To further characterize the influence of Cdk1 on the microtubule binding activity of the Dam1 complex, I performed microtubule co-sedimentation assays with the different phospho-mutants at different MT concentrations (0-5μM). The phospho-mimicking mutants displayed a slight reduction in binding affinity to microtubules as illustrated in the binding curve (Figure 12B) and the corresponding Coomassie-stained gels (Figure 12A).
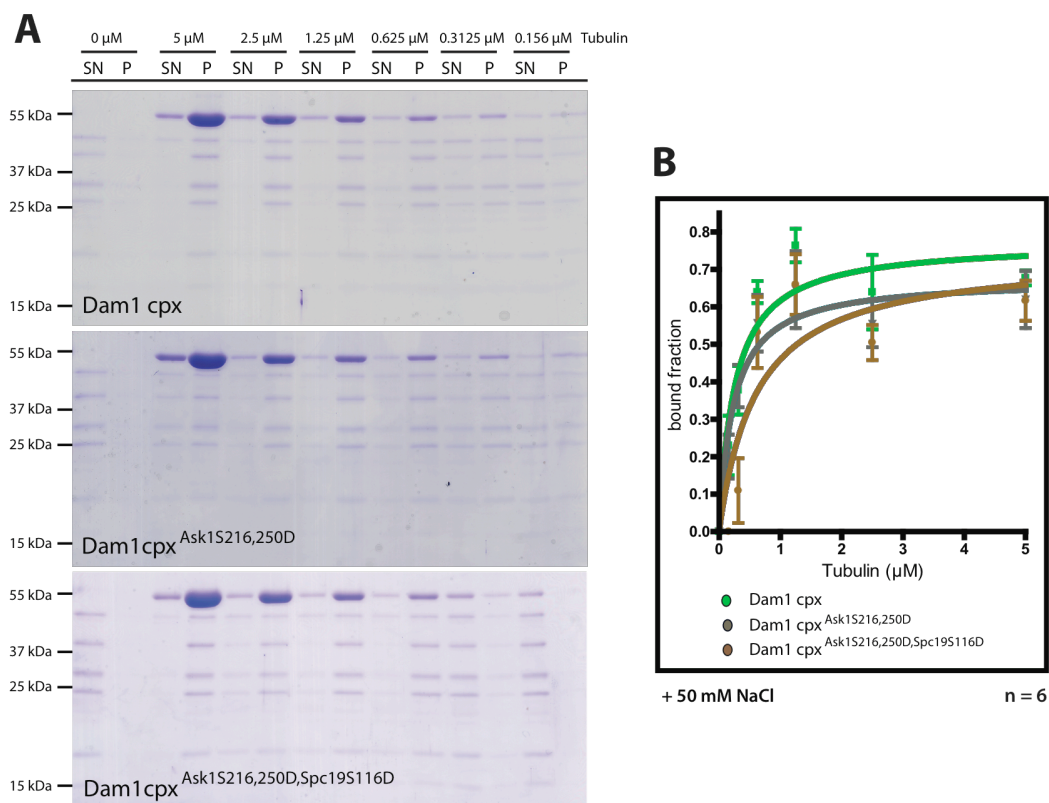
Figure 12: Microtubule-binding assay for phospho-mimicking mutants: B shows the quantification of a series of microtubule binding assays (n=6) using the phospho-mimicking mutants, which show a reduced binding efficiency to microtubules. A illustrates representative Coomassie-stained gels for each mutant.

To confirm this effect under more physiological conditions I pre-phosphorylated the Dam1 WT complex with the kinase and then tested its microtubule binding activity at a given MT concentration (5μM). Under this condition the phenotype was more pronounced (Figure 13).
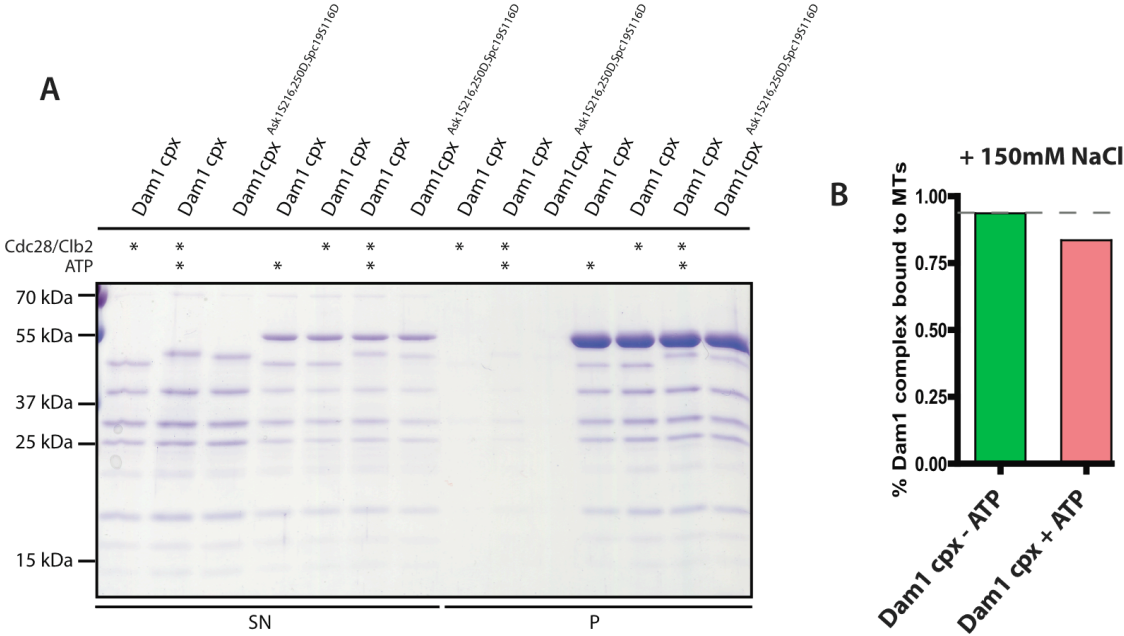
Figure 13: Microtubule-binding assay of *in vitro* phosphorylated Dam1 complex (cpx): The graph in B illustrates the quantification of what is shown in the Coomassie-stained gels (A). Phosphorylation of the Dam1 complex appears to weaken its ability to bind to microtubules.

For the null-mutant I had to modify the microtubule binding procedure using higher salt concentrations (250 mM NaCl). A buffer with increased ionic strength was required because under these conditions the null-mutants are more stable and additionally subtle differences in binding affinities between mutants and WT, which exhibits already a very robust interaction with microtubules, get more strongly pronounced. In contrast to the lowered microtubule binding affinity examined for the phospho-mimicking mutants the phospho-null mutants displayed a rather increased microtubule binding activity (Figure 14).

Figure 14: Microtubule-binding assay for phospho-null mutants: B shows the quantification of a series of microtubule binding assays (n=6) using the phospho-null mutants, which show an increased binding efficiency to microtubules. A illustrates representative Coomassie-stained gels for each mutant.

2.2.5 Recruitment efficiency of Ndc80p to taxol-stabilized microtubules is slightly changed in presence of the phospho-mimicking mutants

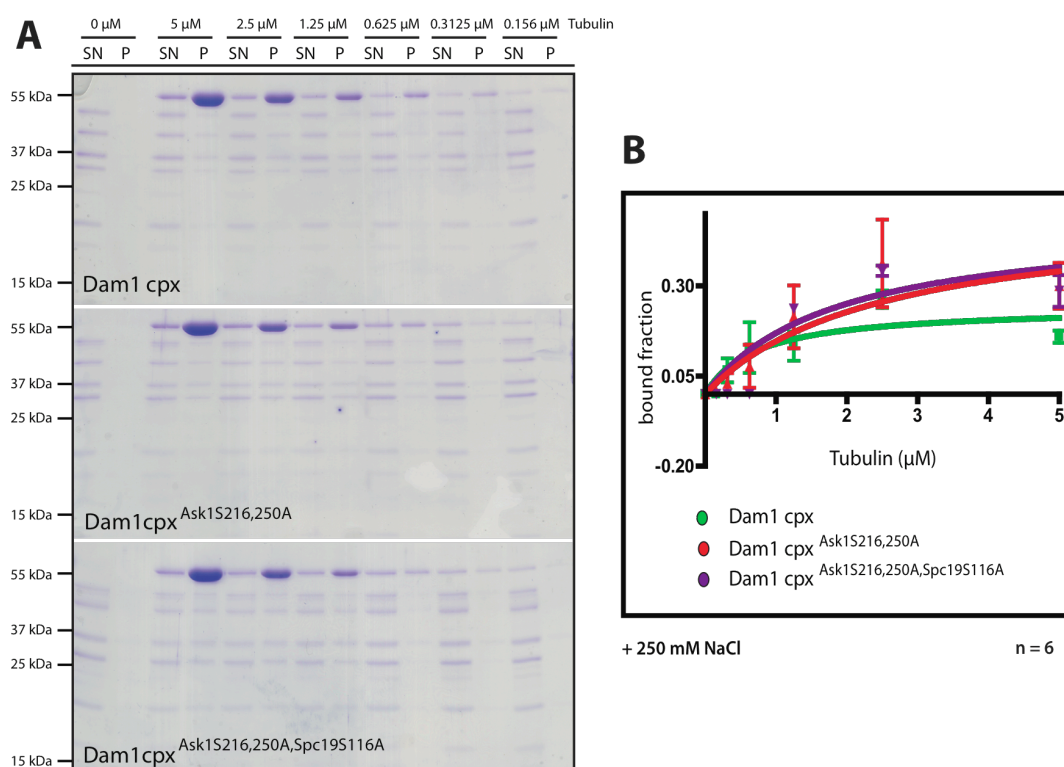It was recently reported that the Dam1 complex increases the affinity of the Ndc80 complex for microtubules. Furthermore it was shown that Ipl1 phosphorylation of the Dam1 complex interferes with its Ndc80 interaction (Lampert et al., 2010; Tien et al., 2010). To examine whether Cdk1 regulation of the Dam1 complex might affect its ability to recruit Ndc80 to microtubules I performed Ndc80-recruitment experiments. Therefore I used equimolar amounts of Ndc80 complex in presence of the Dam1 phospho-mimicking mutants together with taxol-stabilized microtubules. The analysis of the Coomassie-stained gels revealed that the recruited Ndc80 fraction was not significantly reduced in the phospho-mimicking mutants compared to the WT. It is likely that Cdk1 phosphorylation does not interfere with the microtubule-based interaction between Dam1 and Ndc80 (Figure 15).
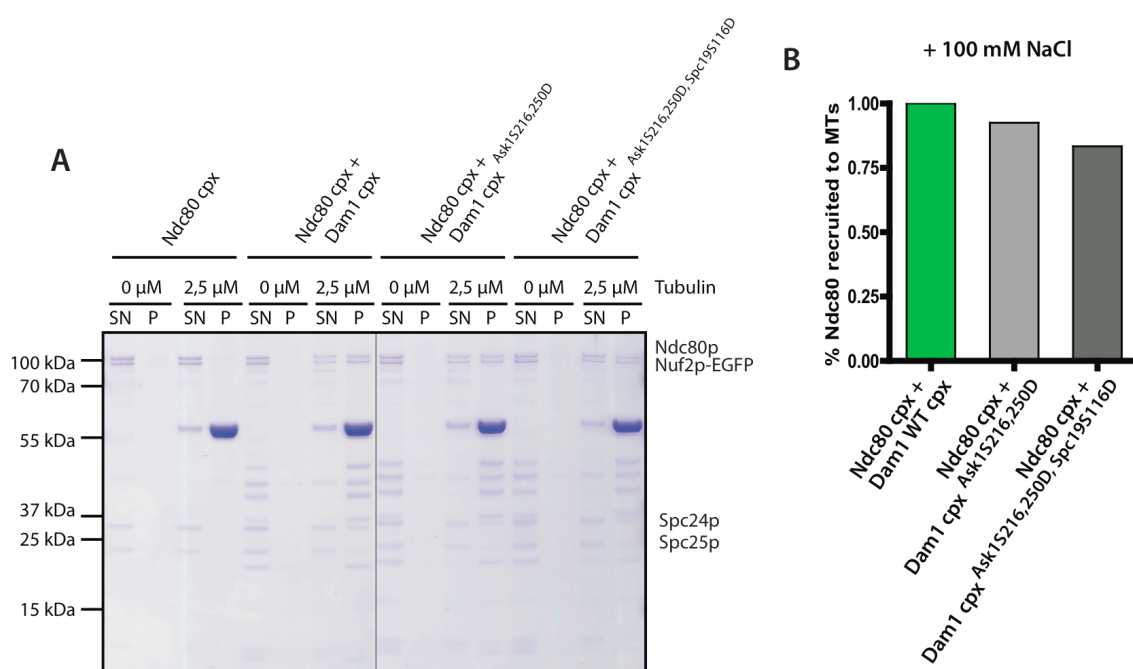
Figure 15: Recruitment of the Ndc80 complex to microtubules by Dam1 phospho-mimicking mutants: The graph in B illustrates the quantification of what is shown in the SDS–polyacrylamide gel stained with Coomassie Brilliant Blue (A). The phospho-mimicking mutants seem to recruit the Ndc80 complex less efficiently to microtubules.

2.2.6 Cdk1-dependent phosphorylation of Dam1 complex lowers ring formation efficiency

Next I wanted to test the ability of the Cdk1-phospho-mutant Dam1 complexes to form rings around taxol-stabilized microtubules. This was of particular interest since it was recently suggested that the C-terminus of Ask1p lies at the interface between two adjacent Dam1 complexes in the ring configuration. Therefore I performed EM analysis of Dam1 ring microtubule decoration. I incubated the different Dam1 complex variants together with taxol-stabilized microtubules to allow ring self-assembly around microtubules. These samples were then further analyzed via negative stain electron microscopy. Both phospho-mutants were able to adopt a ring structure similar to WT complex. However, for the phospho-null mutant I had to increase the protein concentration four fold in order to obtain the same amount of microtubule decoration, probably as a result of the decreased stability of this mutant. For the phospho-mimicking triple mutant no obvious difference in MT decoration could be observed (Figure 16). Therefore I decided to perform an *in vitro* kinase assay of the WT complex prior to the incubation with microtubules, which might mimic a more physiological condition. This experiment revealed decreased microtubule decoration for the phosphorylated complex compared to the unphosphorylated one (Figure 17). The correct control would have been the Dam1 phospho-null mutant, which should be able to restore WT ring formation efficiency under these conditions. Unfortunately it was not possible to test this hypothesis since the alanine-mutant Dam1 complexes are very unstable compared to the WT complex.

Dam1 complex   Dam1 complex ^{Ask1S216,250A,Spc19S116A} Dam1 complex ^{Ask1S216,250D,Spc19S116D}
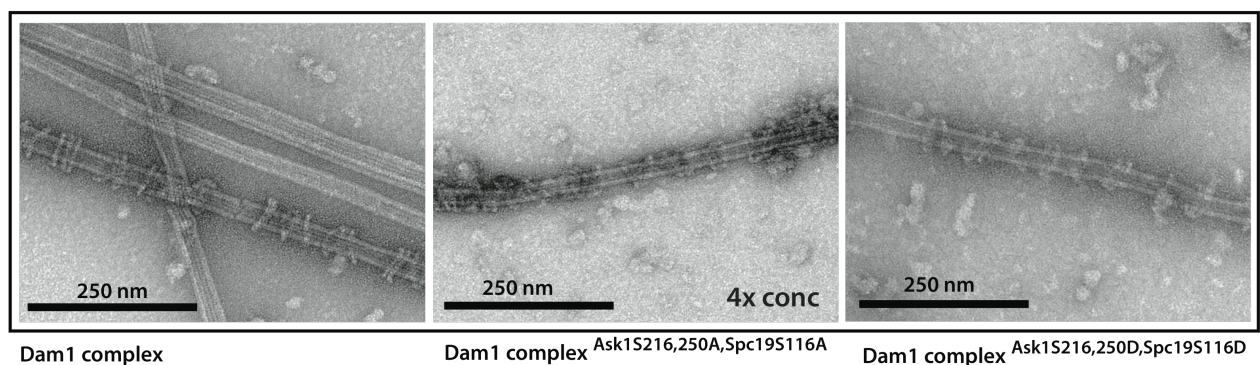
Figure 16: EM analysis of Dam1 ring formation around microtubules: Both triple mutants are able to form rings around microtubules *in vitro*. However, the concentration of the phospho-null mutant needs to be 4 fold increased to be able to form rings.

A unphosphorylated Dam1 complex (- ATP)

phosphorylated Dam1 complex (+ ATP)

250 nm

250 nm

B

Number of Dam1 rings/100nm MT
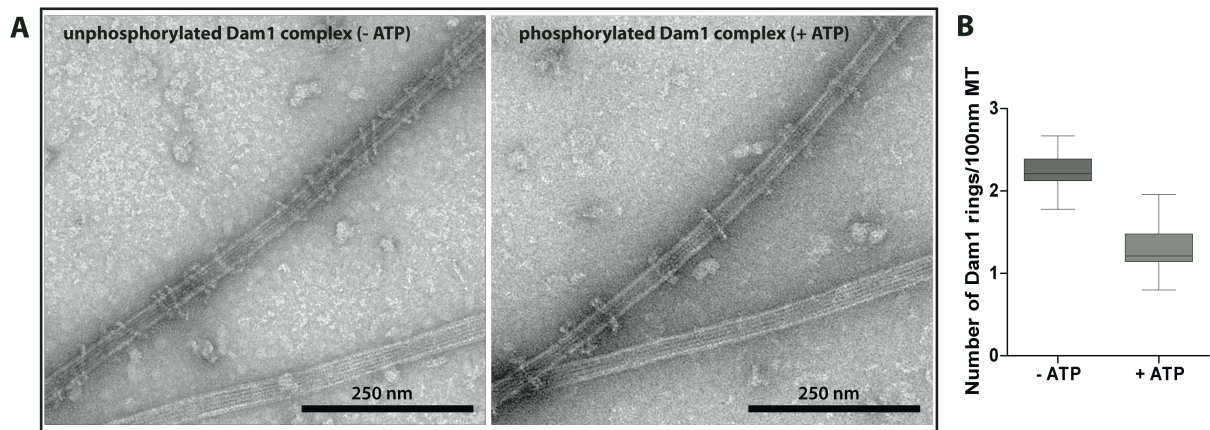
Figure 17: EM analysis of ring formation of *in vitro* phosphorylated Dam1 complex around microtubules: This figure illustrates a decreased ring formation tendency of the phosphorylated Dam1 complex. B represents the quantification of 13 individual microtubules for each condition. A representative micrograph is depicted in panel A.

In summary, Cdk1 phosphorylation does not seem to interfere with Dam1 complex integrity. However, Cdk1 phosphorylated Dam1 complex exhibits a weaker binding affinity for microtubules *in vitro*. Interestingly the phospho-null mutants displayed a more robust interaction with microtubules than the WT complex. We speculated that this effect might arise from the Alanine amino acid-substitutions since the bacteria purified WT Dam1 complex should on its own mimic the non-phosphorylated state. In addition I could show that the phospho-mimicking mutants mildly affect the recruitment efficiency of the Ndc80 complex to microtubules. This is consistent with previous results that Ndc80 rather interacts with Dam1p, which lies on the opposite site of the complex (Lampert et al., 2010; Tien et al., 2010). The slight decrease might be due to the reduced MT binding activity of the mutants themselves.

Interestingly phospho-regulation seems to influence Dam1 inter-complex connections. This is reflected in the decreased ability of the Cdk1-phosphorylated complex to form rings that results in decreased Dam1 ring microtubule decoration.

All together these data suggest that Dam1 complex assembly on microtubules is to some extent regulated by the Cdk1 kinase. To probe whether Cdk1 regulation of the Dam1 complex is an important mechanism *in vivo* I decided to introduce dam1-mutant alleles and characterize them in terms of growth phenotype, spindle dynamics and spindle localization patterns.

2.3 *In vivo* characterization of Dam1 phospho-mutants

It has been reported by Higuchi and co-workers that metaphase microtubule dynamics were highly reduced in the presence of the phospho-null mutant version of Ask1p. This implies a potential mechanism for mitotic spindle stabilization after anaphase onset when Cdc14 dephosphorylates Ask1p. This argument was further strengthened by the observation that after artificially induced anaphase the Ask1 S2A mutant improved chromosome segregation fidelity twofold compared to the WT (Higuchi and Uhlmann, 2005). Consistently my biochemical analysis of the Dam1 complex phospho-mutants revealed enhanced complex-microtubule interaction for the non-phosphorylated state of the complex. To determine whether this specific effect can be correlated with spindle stabilization *in vivo* I decided to perform a detailed *in vivo* characterization.

2.3.1 Dam1 phospho-mutants do not show any growth defects

First I constructed mutants that carry a deletion of the WT ASK1 copy as well as an ASK1 rescue construct, encoding the WT gene product, the double phospho-null mutant or the double phospho-mimicking mutant version. The same strategy was used for generating the Spc19 phospho-mutants. For the generation of the double mutants ASK1/SPC19 I used the ΔSpc19 background with the respective SPC19 rescue construct and replaced ASK1 directly with the different ASK1 variants.

To test whether these mutations compromise growth efficiency all mutant strains were spotted on YPD and YPD + benomyl respectively and incubated at different temperatures ranging from 25 to 37°C. However all mutants phenotypically showed growth rates comparable to the WT control strain (Figure 18).
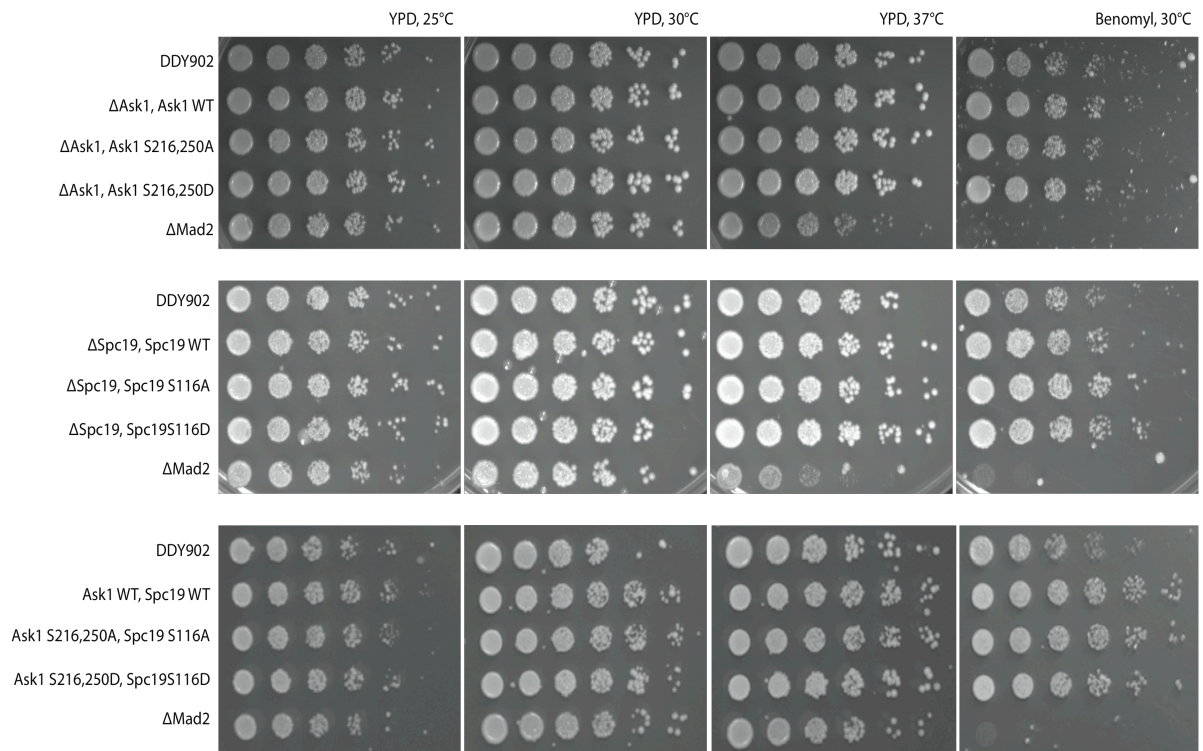
Figure 18: Spot assay of Ask1 phospho-mutants, Spc19-phospho-mutants and double phospho-mutants: all mutants were spotted on YPD and YPD + benomyl plates at different temperatures (25, 30, 34, 37°C). Representative plates are shown in the figure. For none of the mutants an obvious growth defect can be observed. The *Δmad2* allele was used as a control since it is hyper sensitive to benomyl. The strain DDY902 is the WT strain background and was used as positive control.

2.3.2 Different Ask1 phospho-mutants display subtle changes in spindle dynamics

To investigate changes in spindle dynamics I observed anaphase spindle elongation with live-cell microscopy for all different mutants. In order to do so I co-expressed Dad1-GFP that strongly decorates the microtubule lattice and served as the readout for spindle localization. Cells were synchronized in G1 with α-factor and recording of time-lapse movies was started approximately 60 minutes after G1-release, when the cells had entered metaphase, and was stopped after spindle disassembly. Spindle dynamics *per se* during anaphase do not seem to be greatly affected by the Ask1 mutants. The Ask1 phospho-mutants displayed correct anaphase spindle elongation. However, during the "fast phase" of spindle elongation the Ask1 S2A mutant seemed to be faster, while the S2D mutant seemed to be slower than WT Ask1. The "fast phase" of spindle elongation is thought to depend on kinesin-5 motor proteins pushing interpolar microtubules apart (Gerson-Gurwitz et al., 2009; Gheber et al., 1999; Movshovich et al., 2008; Saunders et al., 1995; Straight et al., 1998). This raises the question whether Ask1p influences their function during spindle elongation. Furthermore I could observe that Cdk1-phosphorylated Ask1p reduces overall anaphase duration indicative of slightly enhanced spindle dynamics (figure 19).
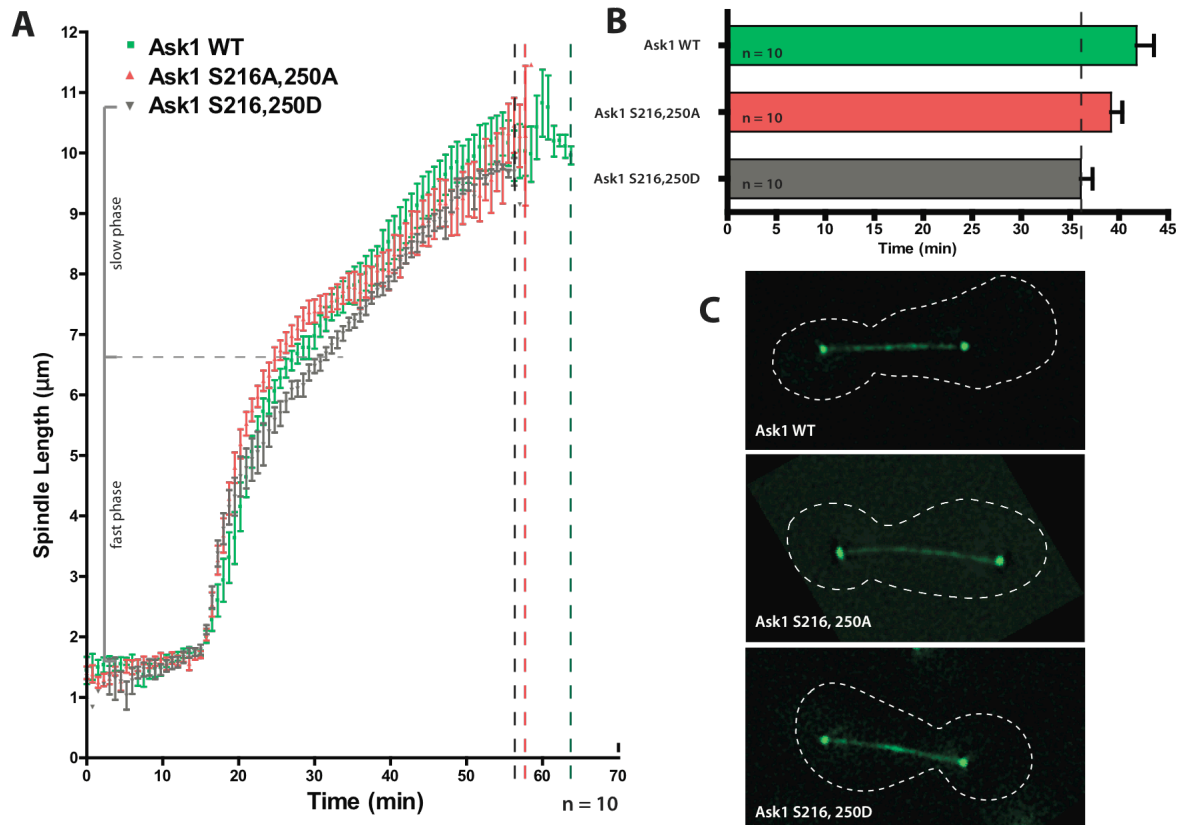
Figure 19: Spindle Dynamics of Ask1 phospho-mutants: Live cell imaging: Images of synchronized cell cultures were recorded every 45 seconds from metaphase until end of anaphase; Graph A illustrates changes in spindle length over time, indicating that the two phospo-mutants have a shorter anaphase than WT (B, C). C represents anaphase spindles for each Ask1 variant.

2.3.3 Ask1 phosphorylation does not affect Dam1 spindle localization

To further examine whether changes in metaphase spindle dynamics correlate with differences in the recruitment efficiency of the Dam1 complex to the metaphase spindle, I quantified the levels of the Dam1 complex at the metaphase spindle and kinetochores respectively. To this end I used live cell microscopy of the metaphase-arrested cells to further measure signal intensities of the Dad1-GFP signal along the entire metaphase spindle. As internal reference I used Nuf2-mCherry, a component of the Ndc80 kinetochore complex. Ask1p phosphorylation does not affect Dam1 spindle localization (Figure 20). Since these measurements include both, the Dam1 population at the spindle and the one at the kinetochore I cannot exclude the possibility that there are differences in the subcellular distribution of Dad1 in the phospho-mutant background. Overall I was not able to detect significant differences in Dad1-GFP levels.
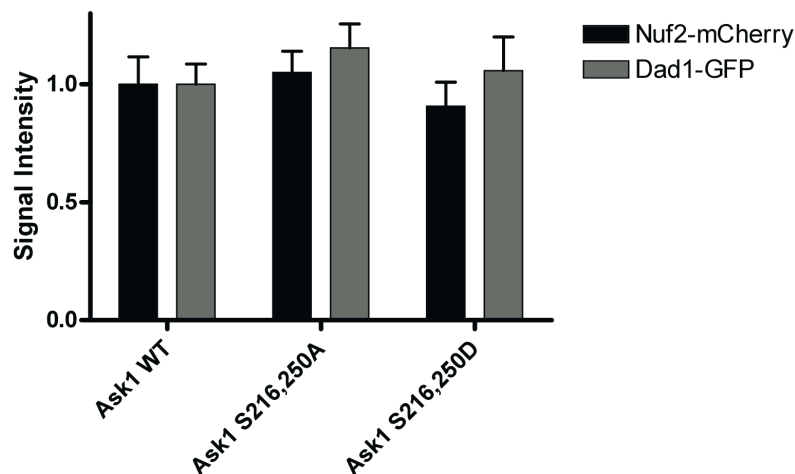
Figure 20: Dam1 complex localization at the metaphase spindle: Signal intensity measurements of Dad1-GFP at the metaphase spindle in metaphase-arrested cells did not demonstrate any relevant differences between the Ask1 phospho-mutants.

2.3.4 The Ask1 phospho-null mutant displays a shorter metaphase spindle and shows an increased spindle localization

It was reported for the Ask1 S2A mutant to decrease microtubule turnover at the metaphase spindle. Therefore I wondered whether the reduction in tubulin turnover might affect metaphase spindle length (Higuchi and Uhlmann, 2005). To analyze this I used the dataset acquired from the intensity measurements in the previous section and measured the distance between the two Nuf2-mCherry signals in each metaphase-arrested cell (Cdc20 arrest). These quantifications revealed a decrease in metaphase spindle length for the non-phosphorylated Ask1 mutant, a result that can be explained by the finding of reduced tubulin turnover at the metaphase spindle for the S2A mutant (Higuchi and Uhlmann, 2005) (Figure 21B). In addition I wanted to investigate whether there is a difference between spindle and kinetochore localization within the different mutants. Therefore I performed line scan measurements. At the kinetochore no obvious differences in Dad1-GFP signal intensities reflecting Dam1 localization could be observed. Interestingly signal intensities along the spindle seemed to be more prominent in the phospho-null mutant (Figure 21A).
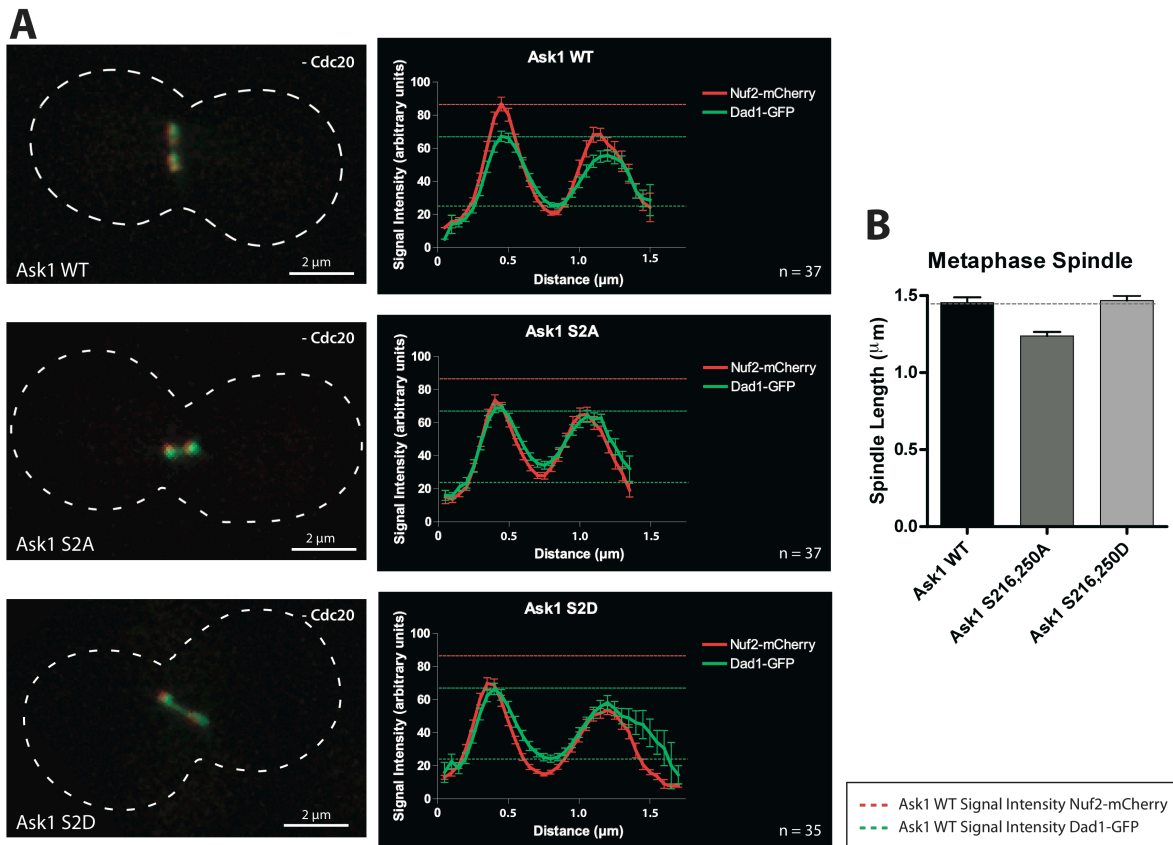
Figure 21: Spindle length measurements and Dam1 complex distribution along the metaphase spindle: A illustrates the distribution of the Dam1 complex along the metaphase spindle. Signal intensities for all three variants are similar at the kinetochore (upper green-dashed line indicates WT levels), whereas the signal along the mitotic spindle seems to be increased in the phospho-null mutant (lower green-dashed line indicates WT levels). B illustrates the significantly decreased metaphase spindle length of the phospho-null mutant.

Taken together the *in vivo* characterization of the Ask1 phospho-null mutant indicates a slight increase in Dam1 complex recruitment to the metaphase spindle, whereas the kinetochore localization does not seem to be affected. Furthermore the metaphase spindle length is significantly reduced in this mutant, which might be due to decreased tubulin turnover as suggested by Higuchi and co-workers. Characterization of Cdk1 phospho-regulation of Spc19p *in vivo* needs to be done in the future.

However, to understand Cdk1 phosphoregulation of Dam1 complex spindle function it might be crucial to include additional regulatory networks such as Ipl1 regulation which was also reported to interfere with Dam1 inter-complex interactions (Ramey et al., 2011).

3 Discussion:

Proper chromosome segregation during cell division depends on the correct and stable attachment of the chromosomes to the mitotic spindle. The major component fulfilling this function is the kinetochore, an elaborate network of protein complexes, with a conserved organization from yeast to human. One of the main elements in the establishment of kinetochore-microtubule attachments in budding yeast is the essential Dam1 kinetochore complex. The Dam1 complex consists of ten subunits and was shown to assemble into a ring-like structure around microtubules *in vitro*, a property that has not yet been confirmed to exist *in vivo* (Cheeseman et al., 2001a; Miranda et al., 2005; Westermann et al., 2005). Dam1 mutants display severe chromosome missegregation *in vivo* and are compromised in the spindle integrity (Cheeseman et al., 2001a; Janke et al., 2002). Although its role in providing correct kinetochore-microtubule attachments and the underlying regulatory mechanisms are quite well understood its contribution to maintenance of spindle integrity during chromosome segregation still remains unclear (Cheeseman et al., 2002; Cheeseman et al., 2001a; Janke et al., 2002; Lampert et al., 2010; Tien et al., 2010). However, recently Higuchi and co-workers suggested a new Cdk1-dependent mechanism regulating one of the Dam1 complex subunits Ask1p (Holt et al., 2009; Li and Elledge, 2003; Ubersax et al., 2003). Because the authors failed in providing a molecular mechanism explaining the observed spindle phenotype, my aim was to gain additional insights into Cdk1-dependent Dam1 phospho-regulation by a comprehensive *in vitro* and *in vivo* study.

3.1 Identification of Cdk1 substrates

Mitotic progression has to be tightly regulated in a temporal and spatial manner. These switch-like mechanisms often rely on posttranslational modifications of various cellular proteins. Protein phosphorylation is the most frequent form of mitotic modification that leads to protein conformational changes, can alter protein functionality or activity and often interferes with protein-protein interactions. Coordination of these events in a biological context depends on the interplay between kinases and their opposing phosphatases. These complex kinase-phosphatase networks regulate many cellular functions, among them proper

43

chromosome segregation and cytokinesis. The Dam1 complex is highly phosphorylated *in vivo* by different mitotic kinases such as Ipl1p, Mps1p and Cdk1p (Cheeseman et al., 2002; Li and Elledge, 2003; Shimogawa et al., 2006). Due to its essential role as a coupler at the outer part of the kinetochore and acting as a direct contact to the mitotic spindle, it needs to be tightly regulated during cell division. Ipl1p and Mps1p directly regulate the Dam1 complex as they were shown to govern the establishment of correct attachments between the kinetochore and the spindle microtubules *in vivo* (Cheeseman et al., 2002; Cheeseman et al., 2001a; Janke et al., 2002; Shimogawa et al., 2006).

Prior to the separation of the two sister chromatids the kinetochore-microtubule attachments are highly dynamic enabling chromosome bi-orientation (Huang and Huffaker, 2006). However, after anaphase onset their dynamics decrease, thereby stabilizing the connections of chromosomes to the spindle. This is accomplished by reversal of Cdk1-dependent kinetochore phosphorylation at the metaphase-to-anaphase transition (Higuchi and Uhlmann, 2005). Several Cdk1 substrates have been identified as being directly involved in the mechanism regulating spindle dynamics. One of them is Sli15p, a well-known Cdk1 substrate, involved in anaphase spindle stabilization and part of the conserved chromosomal passenger complex (CPC). Cdk1-phosphorylation regulates the microtubule binding affinity of Sli15p that when Cdk1 activity is low at anaphase onset, drives relocation of the CPC from the kinetochore to the spindle midzone (Nakajima et al., 2011; Pereira and Schiebel, 2003). Additional substrates such as the microtubule-associated protein Stu1p, the microtubule stabilizing factor Fin1p and the microtubule bundling factor Ase1p were shown to be targeted by Cdk1 and after Cdc14 dephosphorylation promote spindle stability after metaphase-to-anaphase transition (Higuchi and Uhlmann, 2005; Khmelinskii et al., 2009; Woodbury and Morgan, 2007). Dephosphorylated Ase1p and Stu1p are recruited to the spindle midzone, the region of overlapping interpolar-microtubule plus-ends, whereas dephosphorylated Sli15p is first localized to the entire spindle before it gets enriched at the midzone. Dephosphorylated Fin1p was shown to localize all along the anaphase spindle stabilizing the microtubules (Higuchi and Uhlmann, 2005; Khmelinskii et al., 2009; Nakajima et al., 2011; Pereira and Schiebel, 2003; Woodbury and Morgan, 2007). The component involved in the regulation of microtubule dynamics of kinetochore-microtubules has not yet been identified. Interestingly, a recent study suggests that the Dam1 subunit Ask1p, comprising two Cdk1 phospho-sites (S216, S250), might be this missing element as it is directly involved in the control of spindle

behavior (Higuchi and Uhlmann, 2005). It was shown that metaphase spindle dynamics were greatly reduced in presence of Ask1p compromised in Cdk1 phosphorylation, as monitored by decreased tubulin turnover. This finding suggests a role for Ask1p in the mitotic spindle stabilization after anaphase onset. This assumption was supported by the observation that after artificially induced anaphase the Ask1 S2A mutant improved chromosome segregation fidelity twofold (Higuchi and Uhlmann, 2005).

In order to understand the regulatory network underlying Dam1 spindle function I decided to screen for more potential Cdk1 substrates within the Dam1 complex. Mass spec analysis revealed that the subunit Spc19p is an additional potential Cdk1 target *in vivo*. I could confirm the Cdk1 specificity for Spc19p at the position S116, which is situated within a Cdk1 minimal consensus motif (SP), by an *in vitro* kinase assay. This site was then included in my subsequent biochemical analysis of Cdk1 dependent regulation of the Dam1 complex function. This additional phospho-site had only minor effects on the Dam1 complex properties *in vitro* and further did not worsen the growth of Ask1 phospho-mutants *in vivo*.

Besides its function in the regulation of spindle dynamics Cdk1 is known to have an impact on the control of many cell cycle events in a temporal and spatial manner. Furthermore reversing Cdk1 activity by degrading mitotic cyclins and raising Cdc14 activity was shown to be crucial for proper chromosome segregation and mitotic exit (Morgan, 2006; Oliveira et al., 2010). To explore the mechanisms of cell-cycle control by Cdk1 further a global analysis of Cdk1 substrates in *S. cerevisiae* was performed revealing a high number of potential Cdk1 targets (Holt et al., 2009; Ubersax et al., 2003). Specific functions correlating with Cdk1 phospho-regulation are assigned only for a fraction of these substrates, whereas the functions of the bulk of these phospho-regulated proteins remain unclear. Therefore it would be interesting to characterize the role of Cdk1 phospho-regulation for these newly identified substrates in order to shed light on this elaborate regulatory network.

Furthermore, in order to decipher the physiological context of the combination of different kinases acting on specific substrates, which are involved in a cellular process such as the regulation of spindle dynamics, it would be very interesting to determine the phospho-status of these substrates at defined timepoints during the cell cycle. This would allow to really investigate the function and interplay of specific proteins under more physiological conditions in order to get an overall picture of their contribution to a specific mechanism.

3.2 Does Cdk1 regulate Dam1 ring formation?

Properties of the Dam1 complex required for its microtubule binding activity as well as ring formation have been well studied *in vitro* (Janke et al., 2002; Miranda et al., 2005; Westermann et al., 2005). It was shown that the Dam1 complex can reproduce essential aspects of the kinetochore *in vitro* such as plus-end tracking on depolymerizing microtubules and coupling cargoes to microtubules (Asbury et al., 2006; Westermann et al., 2006). The Dam1 ring model explains how the energy of microtubule disassembly is translated into the chromosome movement. It has been shown that the outward peeling of protofilaments pushes the ring and attached cargoes towards the opposite spindle poles (Grishchuk et al., 2008; Westermann et al., 2006). But is there a mechanism to specifically regulate the Dam1 function at the kinetochore and the state of its oligomerization? To understand that I first studied how the Dam1 complex contributes to the regulation of spindle dynamics and how Cdk1 phosphorylation changes its intrinsic properties such as complex integrity, ring formation and microtubule binding affinity. A new mechanistic hint was proposed by Ramey and co-workers suggesting that the C-terminal part of Ask1p harboring the two identified Cdk1 phospho-sites lies within a potential interface responsible for the formation of inter-complex contacts during Dam1 ring formation. They also suggest that Spc19p (among other possible candidates) lies on the other side of the interface but such a direct interaction between Ask1p and Spc19p has not been shown so far (Wong et al., 2007). The N-terminal part of Ask1p was shown to be located in the central region of the complex, where it interacts with other subunits (Ikeuchi et al., 2010; Ramey et al., 2011). To test whether Cdk1 regulation of Ask1p and Spc19p supports the proposed model, I constructed and analyzed recombinant Dam1 complexes, either lacking the potential Cdk1 phospho-sites or mimicking the Cdk1-phosphorylation. The microtubule binding affinity of the complex was decreased after Cdk1 phosphorylation. This finding is surprising as both Ask1p and Spc19p are suggested to be not in direct contact with the microtubule lattice and thereby it cannot be explained by direct electrostatic repulsion between the microtubule surface and the phosphorylated Ask1p or Spc19p subunits (Ramey et al., 2011). Although the Cdk1 activity is thought to interfere with either intra- or inter-complex connections my analysis of Dam1 complex integrity did not reveal any significant differences between the subunit composition of Dam1 phospho-mutants (Ramey et al., 2011). Interestingly, the phosphorylated Dam1 complex displayed a decreased

tendency for ring formation. This observation is consistent with the assumption that Cdk1 phosphorylation of Ask1p at its C-terminus interferes with its ability to oligomerize.

My observations therefore suggest a Cdk1-dependent mechanism regulating Dam1 oligomerization where decreased ring formation correlates with a slight reduction in MT binding. Dam1 decoration of microtubules is a cooperative mechanism resulting in a mixed population of highly decorated and naked microtubules (Gestaut et al., 2008). Furthermore Dam1 oligomerization *per se* depends on the concentration of the complex. Under our experimental conditions using high Dam1 complex concentrations only subtle changes in MT binding affinities could be observed. Thus, conditions where Dam1 complex concentrations are kept low could reveal more severe differences. This could be done by performing quantitative WBs of microtubule binding assays at low Dam1 complex concentrations. In addition, the changes in cooperative binding could be analyzed by TIRF microscopy, which allows to follow oligomerization in real time and to determine parameters such as the Hill coefficient, which provides a quantitative method for the characterization of the binding cooperativity of the complex to microtubules (Gestaut et al., 2008). A strong effect on the cooperativity of binding would be expected if ring formation is impaired.

A similar regulatory principle was proposed for Ipl1-dependent phospho-regulation of the Dam1p and Spc34p subunits, which build up a second interface, referred to as outer interface, connecting two adjacent Dam1 complexes (Ramey et al., 2011). This interaction involves the C-terminal part of the Dam1 subunit as well as Spc34p, which are both phosphorylated by Ipl1p (Dam1 S257D, S265D, S292D; Spc34 T199). The phospho-mimicking mutant of Dam1 has only little effect on its ability to bind to microtubules but reduces the efficiency of ring assembly *in vitro* (Wang et al., 2007; Westermann et al., 2005). Additionally, *in vitro* Ipl1-phosphorylated Dam1 complex cannot form rings around microtubules (Zimniak, Lampert et *al.,* unpublished data), presumably by weakening the interactions between the Spc34p and Dam1p subunits (Ito et al., 2001; Ramey et al., 2011; Shang et al., 2003; Wong et al., 2007). Importantly it was demonstrated that Ipl1-dependent phosphorylation of the Dam1 complex weakens its interaction with the Ndc80 complex *in vivo* and decreases Dam1-dependent Ndc80 microtubule recruitment *in vitro* (Lampert et al., 2010; Shang et al., 2003; Tien et al., 2010). Therefore Ipl1 phospho-regulation influences predominantly the interaction between

Dam1 and Ndc80 complexes but furthermore has an impact together with Cdk1 phospho-regulation on Dam1 ring formation efficiency.

Since I could only observe a slight reduction in Dam1-dependent Ndc80 recruitment to microtubules in presence of the Ask1 phospho-mutants I assume that Cdk1-dependent phospho-regulation of the Dam1 complex does not interfere with this interaction.

To test if the efficiency of ring formation is affected by both Ipl1 and Cdk1 phosphorylation I aimed to purify the Dam1 complex mimicking phosphorylation for both kinases. Despite my efforts, making an S6D Dam1 phospho-mutant was unsuccessful (Miranda et al., 2005). To understand the contribution of the two kinases to Dam1 function it would be more accurate to include the additional Cdk1 phospho-site in Spc19p as well as the Ipl1 phospho-site in Ask1p (Cheeseman et al., 2002). Furthermore *in vitro* phosphorylation of the Dam1 complex by both kinases and subsequently probing for its microtubule binding affinity or microtubule plus-end tracking efficiency could provide insights into the simultaneous phosphorylation by both kinases on Dam1 function. This phospho-status mimics a more physiological context of the complex, since it was shown to be a target of both kinases during metaphase.

It could be speculated that Ipl1 phospho-regulation of the so-called outer interface (including Spc34p and Dam1p) interferes more dramatically with oligomerization and possibly ring formation. In contrast Cdk1-dependent regulation of the inner interface (consisting of Ask1p and probably Spc19p) could affect the stability of the complex structure less severe probably by not affecting the overall oligomerization process but rather stabilizing or tightening the structure around microtubules.

3.3 Consequences of the Cdk1 dependent phosphorylation on the Dam1 complex function *in vivo*

It has been reported that spindle dynamics are decreased under conditions of low Cdk1 activity and that dephosphorylation of the Dam1 subunit Ask1p contributes to spindle stabilization during anaphase (Higuchi and Uhlmann, 2005; Kline-Smith and Walczak, 2004; Maddox et al., 2000; Mallavarapu et al., 1999; Zhai et al., 1995). Interestingly the metaphase spindle length was greatly reduced in the Ask1 S2A mutant, which most likely results from a decreased tubulin turnover as shown by Higuchi and co-workers.

Although most factors regulating the dynamics of the anaphase spindle display a dramatic change in localization pattern at the time of decreased Cdk1 activity we were not able to detect any significant differences in the localization between different Ask1 phospho-mutants along the elongating anaphase spindle. Monitoring Dam1 spindle decoration during metaphase revealed slight differences in Dam1 localization along the spindle, which seemed more prominent for the phospho-null mutant. It was observed that an *ask1-3* temperature sensitive mutants loose Dam1 spindle decoration after chromosome segregation, a defect that has also been observed in *dam1-1* mutants (Cheeseman et al., 2001b; Jones et al., 1999; Li et al., 2002). Since monitoring signal intensities over a longer period of time always leads to bleaching of the fluorophores it is often difficult to detect slight differences in signal intensities between different samples, which are therefore subjected to fluctuations. In order to minimize the bleaching effect and thereby detect slight changes in Dam1 spindle decoration during anaphase for the different mutants it is crucial to monitor their localization pattern at a defined timepoint, enriching for anaphase cells by introducing the *cdc15-2* allele. Since differences in Dam1 spindle decoration could result from a change in the dynamics of the complex it would be interesting to examine Dam1 complex dynamics for the different phospho-mutants. One possibility to do this is by performing FRAP experiments, which could give a direct read-out about complex turnover at the spindle.

In addition, the amount of complex localizing at the kinetochore did not reveal any differences between the phospho-mutants, which is consistent with the fact that Dam1 recruitment to the kinetochore does not only depend on microtubule binding but is also highly affected by its interaction with the Ndc80 complex. Furthermore ring formation around microtubules depends on Dam1 concentration and might be influenced by interaction with the Ndc80 complex through increase of its local enrichment at the kinetochore.

Importantly the Ipl1 phosphorylation mimicking S4D Dam1 complex mutant displays an impaired growth phenotype *in vivo,* whereas the Cdk1 dependent S3D mutant is not compromised in cell viability. This could be due to their differential contribution in the regulation of the Dam1-Ndc80 interaction and the Dam1 oligomerization efficiency *in vivo*. In addition, the combination of Dam1 S4D and Ask1 S2D does not make the cells grow worse compared to the single mutants (data not shown). Since Ipl1 phosphorylation interferes with the interaction between Dam1 and Ndc80 complexes, which is important for stable

kinetochore-microtubule attachments, the effects of Cdk1 on Dam1 function might become negligible. This might be presumably due to the fact that under this perturbed condition the oligomerization state of the Dam1 complex does not influence the chromosome segregation fidelity further.

Altogether the results of my experiments suggest a model by which reversing Cdk1 phosphorylation of the Dam1 complex after anaphase onset increases the efficiency of its oligomerization on microtubules. This is correlated with complex stabilization, an improved spindle integrity as well as decreased spindle dynamics *in vivo*. Furthermore this model also supports the idea of how high Cdk1 activity before anaphase onset provides a highly dynamic spindle needed for the microtubule "search-and-capture" mechanism (Kirschner and Mitchison, 1986). The proposed working model is depicted below (Figure 22).
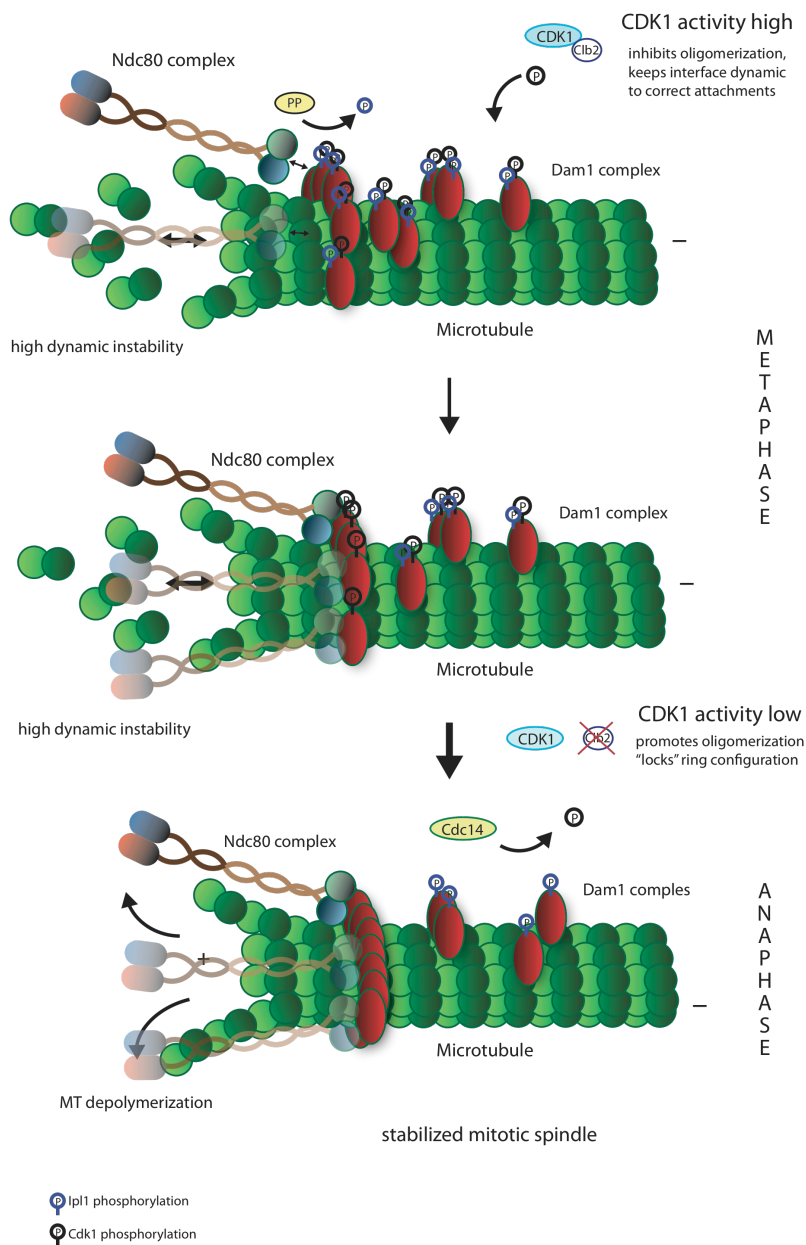
Figure 22: Working model: Phosphorylated Dam1 complexes assemble along the microtubule lattice. Under this condition the mitotic spindle is highly dynamic allowing the microtubules to search and capture kinetochores. Interaction with the Ndc80 complex occurs after dephosphorylation of Dam1p by the responsible phosphatase (PP) inducing oligomerization of the Dam1 ring, still with high order of plasticity required for proper attachments. Dephosphorylation of the Dam1 complexes by Cdc14p after anaphase onset triggers the tightening of the rings around microtubules. Under this condition the mitotic spindle gets stabilized improving chromosome segregation in anaphase A.

4 Material and Methods

4.1 Material

4.1.1 Yeast strains used in this study

Name	Genotype
DDY902	Mat a, ade2-1, leu2-3, his3Δ200, ura3-52
DDY1503	Mat a, his3Δ200, leu2-3,112, ura3-52, ade2-1, Δmad2::URA3
FLY62	Mat a; leu2-3,112, ura3-52, ade2-1, lys2-801, Dad1-TAP::HIS3, pGAL-Cdc20
VFY1	Mat a, tor1-1fpr1::loxP-LEU2-loxP, RPL13A-2xFKBP12::loxP-TRP1-loxP, Ask1-FRB::KanMX
VFY2	Mat a, tor1-1fpr1::loxP-LEU2-loxP, RPL13A-2xFKBP12::loxP-TRP1-loxP
VFY3	Mat a, tor1-1fpr1::loxP-LEU2-loxP, RPL13A-2xFKBP12::loxP-TRP1-loxP, Ask1-FRB-GFP::KanMX
VFY4	Mat a, tor1-1fpr1::loxP-LEU2-loxP, RPL13A-2xFKBP12::loxP-TRP1-loxP, Ask1-FRB::KanMX
VFY5	Mat a, tor1-1fpr1::loxP-LEU2-loxP, RPL13A-2xFKBP12::loxP-TRP1-loxP, Ask1-FRB-GFP::KanMX, pAsk1-WT::HIS3
VFY6	Mat a, tor1-1fpr1::loxP-LEU2-loxP, RPL13A-2xFKBP12::loxP-TRP1-loxP, Ask1-FRB-GFP::KanMX, pAsk1S2A::HIS3
VFY7	Mat a, tor1-1fpr1::loxP-LEU2-loxP, RPL13A-2xFKBP12::loxP-TRP1-loxP, Ask1-FRB-GFP::KanMX, pAsk1S2D::HIS3
VFY8	Mat a, tor1-1fpr1::loxP-LEU2-loxP, RPL13A-2xFKBP12::loxP-TRP1-loxP, Ask1-FRB-GFP::KanMX, pHIS::mCherry-Tub1::URA
VFY9	Mat a, tor1-1fpr1::loxP-LEU2-loxP, RPL13A-2xFKBP12::loxP-TRP1-loxP, Ask1-FRB-GFP::KanMX, pHIS::mCherry-Tub1::URA, pAsk1WT::HIS3
VFY10	Mat a, tor1-1fpr1::loxP-LEU2-loxP, RPL13A-2xFKBP12::loxP-TRP1-loxP, Ask1-FRB-GFP::KanMX, pHIS::mCherry-Tub1::URA
VFY11	Mat a, tor1-1fpr1::loxP-LEU2-loxP, RPL13A-2xFKBP12::loxP-TRP1-loxP, Ask1-FRB-GFP::KanMX, pHIS::mCherry-Tub1::URA, pAsk1WT::HIS3
VFY13	Mat alpha, tor1-1fpr1::loxP-LEU2-loxP, RPL13A-2xFKBP12::loxP-TRP1-loxP, Ask1-FRB::KanMX, pHIS::mCherry-Tub1::URA
VFY14	Mat a, tor1-1fpr1::loxP-LEU2-loxP, RPL13A-2xFKBP12::loxP-TRP1-loxP, Ask1-FRB::KanMX, pDad1-GFP::HIS
VFY15	Mat alpha, tor1-1fpr1::loxP-LEU2-loxP, RPL13A-2xFKBP12::loxP-TRP1-loxP, Ask1-FRB::KanMX, pHIS::mCherry-Tub1::URA, pAsk1-WT::HIS3
VFY16	Mat alpha, tor1-1fpr1::loxP-LEU2-loxP, RPL13A-2xFKBP12::loxP-TRP1-loxP, Ask1-FRB::KanMX, pHIS::mCherry-Tub1::URA, pAsk1-S2A::HIS3
VFY17	Mat alpha, tor1-1fpr1::loxP-LEU2-loxP, RPL13A-2xFKBP12::loxP-TRP1-loxP, Ask1-FRB::KanMX, pHIS::mCherry-Tub1::URA, pAsk1-S2D::HIS3
VFY18	Mat a, tor1-1fpr1::loxP-LEU2-loxP, RPL13A-2xFKBP12::loxP-TRP1-loxP, Spc19-FRB::KanMX
VFY19	Mat a, tor1-1fpr1::loxP-LEU2-loxP, RPL13A-2xFKBP12::loxP-TRP1-loxP, Ask1-FRB::KanMX, pHIS::GFP-Tub1::HIS3
VFY20	Mat a, tor1-1fpr1::loxP-LEU2-loxP, RPL13A-2xFKBP12::loxP-TRP1-loxP, Ask1-FRB::KanMX, pHIS::GFP-Tub1::HIS3, pAsk1-WT::URA
VFY21	Mat a, tor1-1fpr1::loxP-LEU2-loxP, RPL13A-2xFKBP12::loxP-TRP1-loxP, Ask1-FRB::KanMX, pHIS::GFP-Tub1::HIS3, pAsk1-S2A::URA
VFY22	Mat a, tor1-1fpr1::loxP-LEU2-loxP, RPL13A-2xFKBP12::loxP-TRP1-loxP, Ask1-

	FRB::KanMX, pHIS::GFP-Tub1::HIS3, pAsk1-S2D::URA
VFY23	Mat a, tor1-1fpr1::loxP-LEU2-loxP, RPL13A-2xFKBP12::loxP-TRP1-loxP, Spc19-FRB::KanMX, pSpc19-WT::HIS3
VFY24	Mat a, tor1-1fpr1::loxP-LEU2-loxP, RPL13A-2xFKBP12::loxP-TRP1-loxP, Spc19-FRB::KanMX, pSpc19-S1A::HIS3
VFY25	Mat alpha, tor1-1fpr1::loxP-LEU2-loxP, RPL13A-2xFKBP12::loxP-TRP1-loxP, Ask1-FRB::KanMX
VFY26	Mat alpha, tor1-1fpr1::loxP-LEU2-loxP, RPL13A-2xFKBP12::loxP-TRP1-loxP, Ask1-FRB::KanMX, pAsk1-WT::HIS3
VFY27	Mat a, tor1-1fpr1::loxP-LEU2-loxP, RPL13A-2xFKBP12::loxP-TRP1-loxP, Ask1-FRB::KanMX, pAsk1-WT::HIS3
VFY28	Mat a, tor1-1fpr1::loxP-LEU2-loxP, RPL13A-2xFKBP12::loxP-TRP1-loxP, Ask1-FRB::KanMX, pAsk1-S2A::HIS3
VFY29	Mat a, tor1-1fpr1::loxP-LEU2-loxP, RPL13A-2xFKBP12::loxP-TRP1-loxP, Ask1-FRB::KanMX, pAsk1-S2D::HIS3
VFY30	Mat a/alpha, Ade2/ade2-1, his3Δ200/his3Δ200, leu2-3,112/leu2-3,112, ura3-52/ura3-52, Lys2/lys2-801, ask1Δ::KanMX
VFY31	Mat a, tor1-1fpr1::loxP-LEU2-loxP, RPL13A-2xFKBP12::loxP-TRP1-loxP, Spc19-FRB::KanMX, pSpc19-S1D::HIS3
VFY32	Mat a, ade2-1, leu2-3,112, his3Δ200, ura3-52, pSpc19-3xHA::KanMx
VFY33	Mat alpha, tor1-1fpr1::loxP-LEU2-loxP, RPL13A-2xFKBP12::loxP-TRP1-loxP, Ask1-FRB::KanMX, ade2-1, promURA3::tetR::GFP-LEU2, tetOx112-URA3
VFY34	Mat a/alpha, Ade2/ade2-1, his3Δ200/his3Δ200, leu2-3,112/leu2-3,112, ura3-52/ura3-52, Lys2/lys2-801, ask1Δ::KanMX, spc19Δ::URA3
VFY35	Mat a/alpha, Ade2/ade2-1, his3Δ200/his3Δ200, leu2-3,112/leu2-3,112, ura3-52/ura3-52, Lys2/lys2-801, spc19Δ::URA3
VFY36	Mat a, ade2-1, leu2-3,112, his3Δ200, ura3-52, pSpc19-3xHA::KanMx, Pds1-13xmyc::LEU2
VFY37	Mat a, ura3-1, leu2-3,112, trp1-1, his3,11,15, ade2-1, can1-100, cdc28-as1, Spc19-3xHA::KanMx
VFY38	Mat a or alpha, his3D200, ura3-52-, leu2-3,112, cdc14-1, Spc19-3xHA::KanMx
VFY39	Mat a, tor1-1fpr1::loxP-LEU2-loxP, RPL13A-2xFKBP12::loxP-TRP1-loxP, Ask1-FRB::KanMX, pDad1-GFP::HIS, pAsk1-WT::URA3
VFY40	Mat a, tor1-1fpr1::loxP-LEU2-loxP, RPL13A-2xFKBP12::loxP-TRP1-loxP, Ask1-FRB::KanMX, pDad1-GFP::HIS, pAsk1-S2A::URA3
VFY41	Mat a, tor1-1fpr1::loxP-LEU2-loxP, RPL13A-2xFKBP12::loxP-TRP1-loxP, Ask1-FRB::KanMX, pDad1-GFP::HIS, pAsk1-S2D::URA3
VFY42	Mat a/alpha, Ade2/ade2-1, his3Δ200/his3Δ200, leu2-3,112/leu2-3,112, ura3-52/ura3-52, Lys2/lys2-801, ask1Δ::KanMX, pAsk1-WT::URA3
VFY43	Mat a/alpha, Ade2/ade2-1, his3Δ200/his3Δ200, leu2-3,112/leu2-3,112, ura3-52/ura3-52, Lys2/lys2-801, ask1Δ::KanMX, pAsk1-S2A::URA3
VFY44	Mat a/alpha, Ade2/ade2-1, his3Δ200/his3Δ200, leu2-3,112/leu2-3,112, ura3-52/ura3-52, Lys2/lys2-801, ask1Δ::KanMX, pAsk1-S2D::URA3
VFY45	Mat a/alpha, Ade2/ade2-1, his3Δ200/his3Δ200, leu2-3,112/leu2-3,112, ura3-52/ura3-52, Lys2/lys2-801, spc19Δ::URA3, pSpc19-S1A::HIS3
VFY46	Mat a/alpha, Ade2/ade2-1, his3Δ200/his3Δ200, leu2-3,112/leu2-3,112, ura3-52/ura3-52, Lys2/lys2-801, spc19Δ::URA3, pSpc19-S1D::HIS3
VFY47	Mat a, ura3-1, leu2-3,112, trp1-1, his3,11,15, ade2-1, can1-100, cdc28-as1, Spc19-3xHA::KanMx, Pds1-13xmyc::LEU2
VFY48	Mat a or alpha, his3D200, ura3-52-, leu2-3,112, cdc14-1, Spc19-3xHA::KanMx, Pds1-13xmyc::LEU2
VFY49	Mat a/alpha, Ade2/ade2-1, his3Δ200/his3Δ200, leu2-3,112/leu2-3,112, ura3-52/ura3-52, Lys2/lys2-801, spc19Δ::URA3, pSpc19-WT::HIS3
VFY50	Mat a his3Δ200, leu2-3,112, ura3-52, ask1Δ::KanMX, pAsk1-WT::URA3
VFY51	Mat alpha, his3Δ200, leu2-3,112, ura3-52, lys2-801, ask1Δ::KanMX, pAsk1-WT::URA3
VFY52	Mat a, his3Δ200, leu2-3,112, ura3-52, lys2-801, ask1Δ::KanMX, pAsk1-S2A::URA3

VFY53	Mat alpha, his3Δ200, leu2-3,112, ura3-52, lys2-801, ask1Δ::KanMX, pAsk1-S2D::URA3
VFY54	Mat a, his3Δ200, leu2-3,112, ura3-52, lys2-801, ask1Δ::KanMX, pAsk1-S2D::URA3
VFY55	Mat a/alpha, Ade2/ade2-1, his3Δ200/his3Δ200, leu2-3,112/leu2-3,112, ura3-52/ura3-52, Lys2/lys2-801, spc19Δ::URA3, pSpc19-WT::HIS3, ask1Δ::KanMX
VFY56	Mat a/alpha, Ade2/ade2-1, his3Δ200/his3Δ200, leu2-3,112/leu2-3,112, ura3-52/ura3-52, Lys2/lys2-801, spc19Δ::URA3, pSpc19-S1A::HIS3, ask1Δ::KanMX
VFY57	Mat a/alpha, Ade2/ade2-1, his3Δ200/his3Δ200, leu2-3,112/leu2-3,112, ura3-52/ura3-52, Lys2/lys2-801, ask1Δ::KanMX, spc19Δ::URA3, pAsk1-S2D::LEU2
VFY58	Mat a/alpha, Ade2/ade2-1, his3Δ200/his3Δ200, leu2-3,112/leu2-3,112, ura3-52/ura3-52, Lys2/lys2-801, spc19Δ::URA3, pSpc19-S1A::HIS3, ask1Δ::KanMX, pAsk1-S2A::LEU2
VFY59	Mata/alpha, Ade2/ade2-1, his3Δ200/his3Δ200, leu2-3,112/leu2-3,112, ura3-52/ura3-52, Lys2/lys2-801, ask1Δ::KanMX, spc19Δ::URA3, pAsk1-S2D::LEU2, pSpc19-S1D::HIS3
VFY64	Mat a, leu2-3,112, ura3-52, ask1Δ::KanMX, pAsk1-WT::URA3, Dad1-GFP::HIS3
VFY65	Mat a, leu2-3,112, ura3-52, lys2-801, ask1Δ::KanMX, pAsk1-S2A::URA3, Dad1-GFP::HIS3
VFY66	Mat a, leu2-3,112, ura3-52, lys2-801, ask1Δ::KanMX, pAsk1-S2D::URA3, Dad1-GFP::HIS3
VFY68	Mat a, Ade2, lys2-801, ask1Δ::KanMX, spc19Δ::URA3, pAsk1-S2D::LEU2, pSpc19-S1D::HIS3
VFY69	Mat alpha, Ade2, Lys2, ask1Δ::KanMX, spc19Δ::URA3, pAsk1-S2D::LEU2, pSpc19-S1D::HIS3
VFY70	Mat a/alpha, Ade2/ade2-1, his3Δ200/his3Δ200, leu2-3,112/leu2-3,112, ura3-52/ura3-52, Lys2/lys2-801, spc19Δ::URA3, pSpc19-WT::LEU2
VFY71	Mat a/alpha, Ade2/ade2-1, his3Δ200/his3Δ200, leu2-3,112/leu2-3,112, ura3-52/ura3-52, Lys2/lys2-801, spc19Δ::URA3, pSpc19-S1D::LEU2
VFY72	Mata/alpha, Ade2/ade2-1, his3Δ200/his3Δ200, leu2-3,112/leu2-3,112, ura3-52/ura3-52, Lys2/lys2-801, spc19Δ::URA3, pSpc19-S1A::LEU2
VFY73	Mat alpha, Ade2, leu2-3,112, his3Δ200, ura3-52, pAsk1-WT-3xHA::KanMx
VFY74	Mat alpha, Ade2, leu2-3,112, his3Δ200, ura3-52, pSpc19-WT-13xmyc::KanMx
VFY75	Mat a, Ade2, lys2-801, his3Δ200, spc19Δ::URA3, Spc19-WT::LEU2
VFY76	Mat alpha, Ade2, lys2-801, his3Δ200, spc19Δ::URA3, Spc19-WT::LEU2
VFY77	Mat a, ade2-1, Lys2, his3Δ200, spc19Δ::URA3, Spc19-S1A::LEU2
VFY78	Mat alpha, Ade2, Lys2, his3Δ200, spc19Δ::URA3, Spc19-S1A::LEU2
VFY79	Mat a, Ade2, Lys2, his3Δ200, spc19Δ::URA3, Spc19-S1D::LEU2
VFY80	Mat alpha, Ade2, Lys2, his3Δ200, spc19Δ::URA3, Spc19-S1D::LEU2
VFY81	Mat alpha, Ade2, leu2-3,112, his3Δ200, ura3-52, pAsk1-S2D-3xHA::KanMx
VFY82	Mat alpha, Ade2, leu2-3,112, his3Δ200, ura3-52, pSpc19-S1A-13xmyc::KanMx
VFY83	Mat alpha, Ade2, leu2-3,112, his3Δ200, ura3-52, pAsk1-S2A-3xHA::KanMx
VFY84	Mat alpha, Ade2, leu2-3,112, his3Δ200, ura3-52, pSpc19-S1D-13xmyc::KanMx
VFY85	Mat a/alpha, Ade2/ade2-1, his3Δ200/his3Δ200, leu2-3,112/leu2-3,112, ura3-52/ura3-52, Lys2/lys2-801, spc24Δ::LEU2
VFY86	Mat a, Ade2, lys2-801, his3Δ200, ΔSpc19::URA3, Spc19-WT::LEU2, Ask1-WT-3xHA::KanMX
VFY87	Mat alpha, Ade2, Lys2, his3Δ200, ΔSpc19::URA3, Spc19-S1A::LEU2, Ask1-S2A-3xHA::KanMX
VFY88	Mat a, Ade2, Lys2, his3Δ200, ΔSpc19::URA3, Spc19-S1D::LEU2, Ask1-S2D-3xHA::KanMX
VFY92	Mat alpha, leu2-3,112, his3Δ200, ura3-52, pHIS:GFP-Tub1::HIS3
VFY93	Mat alpha, Ade2, leu2-3,112, his3Δ200, ura3-52, pAsk1-WT-3xHA::KanMx, GFP-Tub1::URA3
VFY94	Mat alpha, Ade2, leu2-3,112, his3Δ200, ura3-52, pAsk1-S2A-3xHA::KanMx, GFP-Tub1::URA3
VFY95	Mat alpha, Ade2, leu2-3,112, his3Δ200, ura3-52, pAsk1-S2D-3xHA::KanMx, GFP-

	Tub1::URA3
VFY96	Mat alpha, Ade2, leu2-3,112, his3Δ200, ura3-52, pSpc19-WT-13xmyc::KanMx, GFP-Tub1::URA3
VFY97	Mat alpha, Ade2, leu2-3,112, his3Δ200, ura3-52, pSpc19-S1A-13xmyc::KanMx, GFP-Tub1::URA3
VFY98	Mat alpha, Ade2, leu2-3,112, his3Δ200, ura3-52, pSpc19-S1D-13xmyc::KanMx, GFP-Tub1::URA3
VFY99	Mat a, tor1-1fpr1::loxP-LEU2-loxP, RPL13A-2xFKBP12::loxP-TRP1-loxP, Ipl1-FRB::KanMX
VFY100	Mat a, Ade2, lys2-801, spc19Δ::URA3, Spc19-WT::LEU2, Dad1-GFP::HIS3
VFY101	Mat a, ade2-1, Lys2, spc19Δ::URA3, Spc19-S1A::LEU2, Dad1-GFP::HIS3
VFY102	Mat a, Ade2, Lys2, spc19Δ::URA3, Spc19-S1D::LEU2, Dad1-GFP::HIS3
VFY103	Mat a, Ade2, his3Δ200, spc24Δ::LEU2, Spc24-WT::URA
VFY104	Mat a, Ade2, his3Δ200, spc24Δ::LEU2, Spc24-S2A::URA
VFY105	Mat a, Ade2, his3Δ200, spc24Δ::LEU2, Spc24-S2D::URA
VFY106	Mat alpha, Ade2, his3Δ200, ura3-52, lys2-801, Pds1-13xmyc::LEU2
VFY107	Mat a, tor1-1fpr1::loxP-LEU2-loxP, RPL13A-2xFKBP12::loxP-TRP1-loxP, Ipl1-FRB::KanMX, Ipl1-WT::URA3
VFY108	Mat a, leu2-3,112, his3Δ200, Ade2, Ask1-KO::KanMX, pAsk1-S2D::URA3, dam1 (S20D, S257D, S265D, S292D)::KanMX
VFY109	Mat alpha, lys2-801am, leu2-3,112, his3D200, ura3-52, GFP-Tub1::URA3, Spc19 WT-3xHA::KanMX
VFY110	Mat alpha, lys2-801am, leu2-3,112, his3D200, ura3-52, GFP-Tub1::URA3, Spc19 S1A-3xHA::KanMX
VFY111	Mat alpha, lys2-801am, leu2-3,112, his3D200, ura3-52, GFP-Tub1::URA3, Spc19 S1D-3xHA::KanMX
VFY112	Mat a, tor1-1fpr1::loxP-LEU2-loxP, RPL13A-2xFKBP12::loxP-TRP1-loxP, Ipl1-FRB::KanMX, Pds1-13xmyc::LEU2
VFY113	Mat a, tor1-1fpr1::loxP-LEU2-loxP, RPL13A-2xFKBP12::loxP-TRP1-loxP, Ipl1-FRB::KanMX, Ipl1 WT::URA3, Pds1-13xmyc::LEU2
VFY114	Mat a, ade2-1, his3Δ200, ura3-52, lys2-801am, Nuf2-mCherry::KanMx, cdc15-2::LEU2
VFY115	Mat alpha, ade2-1, his3Δ200, ura3-52, lys2-801am, Nuf2-mCherry::KanMx, cdc15-2::LEU2
VFY116	Mat a, Ade2, leu2-3,112, his3Δ200, ura3-52, pAsk1-WT-3xHA::KanMx, GFP-Tub1::URA3
VFY117	Mat a, Ade2, lys2-801am, leu2-3,112, his3Δ200, ura3-52, pAsk1-S2A-3xHA::KanMx, GFP-Tub1::URA3
VFY118	Mat a, Ade2, leu2-3,112, his3Δ200, ura3-52, pAsk1-S2D-3xHA::KanMx, GFP-Tub1::URA3
VFY119	Mat a, Ade2, lys2-801am, leu2-3,112, ask1Δ::KanMX, pAsk1-WT::URA3, Dad1-GFP::HIS3, Nuf2-mCherry::KanMX
VFY120	Mat a, Ade2, lys2-801am, leu2-3,112, ask1Δ::KanMX, pAsk1-S2A::URA3, Dad1-GFP::HIS3, Nuf2-mCherry::KanMX
VFY121	Mat a, Ade2, lys2-801am, leu2-3,112, ask1Δ::KanMX, pAsk1-S2D::URA3, Dad1-GFP::HIS3, Nuf2-mCherry::KanMX
VFY122	Mat a/alpha, Ade2/ade2-1, his3Δ200/his3Δ200, leu2-3,112/leu2-3,112, ura3-52/ura3-52, Lys2/lys2-801, ipl1Δ::KanMX
VFY123	Mat a, Ade2, lys2-801am, ask1Δ::KanMX, pAsk1-WT::URA3, Dad1-GFP::HIS3, Nuf2-mCherry::KanMX, cdc15-2::LEU2
VFY124	Mat a, Ade2, lys2-801am, ask1Δ::KanMX, pAsk1-S2A::URA3, Dad1-GFP::HIS3, Nuf2-mCherry::KanMX, cdc15-2::LEU2
VFY125	Mat a, Ade2, lys2-801am, ask1Δ::KanMX, pAsk1-S2D::URA3, Dad1-GFP::HIS3, Nuf2-mCherry::KanMX, cdc15-2::LEU2
VFY126	Mat a/alpha, Ade2/ade2-1, his3Δ200/his3Δ200, leu2-3,112/leu2-3,112, ura3-52/ura3-52, Lys2/lys2-801, Ipl1-degron::URA3, ipl1Δ::KanMX

VFY127	Mat a, Ade2, lys2-801am, leu2-3,112, ask1Δ::KanMX, pAsk1-WT::URA3, Dad1-GFP::HIS3, Nuf2-mCherry::KanMX, pGal::Cdc20::Clonat
VFY128	Mat a, Ade2, lys2-801am, leu2-3,112, ask1Δ::KanMX, pAsk1-S2A::URA3, Dad1-GFP::HIS3, Nuf2-mCherry::KanMX, pGal::Cdc20::Clonat
VFY129	Mat a, Ade2, lys2-801am, leu2-3,112, ask1Δ::KanMX, pAsk1-S2D::URA3, Dad1-GFP::HIS3, Nuf2-mCherry::KanMX, pGal::Cdc20::Clonat
VFY130	Mat a/alpha, Ade2/ade2-1, his3Δ200/his3Δ200, leu2-3,112/leu2-3,112, ura3-52/ura3-52, Lys2/lys2-801, Ipl1-degron::URA3, ipl1Δ::KanMX, Pds1-13xmyc::LEU2
VFY131	Mat a, ade2-1, his3Δ200, Lys2, Ipl1-degron::URA3, ipl1Δ::KanMX, Pds1-13xmyc::LEU2

4.1.2 Plasmids used in this study

Name	Description
pVF2	pAsk1 S2A in pRS303 inDH5α
pVF3	pAsk1 S1A in pRS303 in DH5α
pVF4	pAsk1 S1D in pRS303 in DH5α
pVF5	pAsk1 S2D in pRS303 in DH5α
pVF6	pAsk1 S1E in pRS303 in DH5α
pVF7	pAsk1 in pRS303 in DH5α
pVF8	pC43 hsk3 6xhis in DH5α
pVF9	pC43 hsk3 6xhis, Ask1 S250E in DH5α
pVF10	pSpc19 S1A in pRS303 in DH5α
pVF11	pSpc19 S1D in pRS303 in DH5α
pVF12	pSpc19 S1E in pRS303 in DH5α
pVF13	pAsk1 S2E in pRS303 in DH5α
pVF14	pSpc19 in pRS303 in DH5α
pVF15	pAsk1 WT in pRS305 inDH5α
pVF16	pAsk1 S2A in pRS305 inDH5α
pVF17	pAsk1 S2D in pRS305 inDH5α
pVF18	pSpc19 WT in pRS306 in DH5α
pVF19	pSpc19 S1A in pRS306 in DH5α
pVF20	pSpc19 S1D in pRS306 in DH5α
pVF21	pAsk1 WT in pRS306 inDH5α
pVF22	pAsk1 S2A in pRS306 inDH5α
pVF23	pAsk1 S2D in pRS306 inDH5α
pVF24	pC43 hsk3 6xhis_ Ask1 S250A in Rosetta
pVF25	pC43 hsk3 6xhis_ WT in Rosetta
pVF26	pC43 hsk3 6xhis_Ask1 S250A in XL10Gold
pVF27	pC43 hsk3 6xhis_Ask1 S250A in DH5α
pVF28	pC43 hsk3 6xhis_Ask1 S250D in DH5α
pVF29	pC43 hsk3 6xhis_Ask1 S250A S216A in XL10Gold
pVF30	pC43 hsk3 6xhis_Ask1 S250A S216A, Spc19 S116A in XL10Gold
pVF31	pC43 hsk3 6xhis_ Ask1 S250D in XL10Gold
pVF32	pC43 hsk3 6xhis_ Ask1 S250D S216D in XL10Gold
pVF33	pC43 hsk3 6xhis_ Ask1 S250D S216D, Spc19 S116D in XL10Gold
pVF34	pC43 hsk3 6xhis_Ask1 S250A S216A in Rosetta
pVF35	pC43 hsk3 6xhis_Ask1 S250A S216A, Spc19 S116A in Rosetta

pVF36	pC43 hsk3 6xhis_ Ask1 S250D in Rosetta
pVF37	pC43 hsk3 6xhis_Ask1 S250A S216A in XL10Gold
pVF38	pC43 hsk3 6xhis_Ask1 S250A S216A, Spc19 S116A in XL10Gold
pVF39	pC43 hsk3 6xhis_Ask1 S250D S216D in XL10Gold
pVF40	pC43 hsk3 6xhis_Ask1 S250D S216D, Spc19 S116D in XL10Gold
pVF41	pC43 hsk3 6xhis_Ask1 S250D S216D in Rosetta
pVF42	pC43 hsk3 6xhis_Ask1 S250D S216D, Spc19 S116D in Rosetta
pVF43	pC43 hsk3 6xhis, Dam1 S4D (S20D S257D S265D S292D) complex in XL10Gold
pVF44	pBS SK+ in DH5α
pVF45	pBS SK+, 3' Ask1 WT in XL10Gold
pVF46	pBS SK+, 3' Ask1 S2A in XL10Gold
pVF47	pBS SK+, 3' Ask1 WT + LEU2 in XL10Gold
pVF48	pBS SK+, 3' Ask1 S2A + LEU2 in XL10Gold
pVF49	pBS SK+, 3' Ask1 S2D in XL10Gold
pVF50	pBS SK+, 3' Ask1 S2D + LEU2 in XL10Gold
pVF51	pML7 + Ask1-WT-3xHA in DH5α
pVF52	pML7 + Ask1-S2A-3xHA in DH5α
pVF53	pML7 + Ask1-S2D-3xHA in DH5α
pVF54	pML12 + Spc19 WT-13xmyc in DH5α
pVF55	pML12 + Spc19 S1A-13xmyc in DH5α
pVF56	pML12 + Spc19 S1D-13xmyc in DH5α
pVF57	pSpc19 in pRS305 in DH5α
pVF58	pSpc19 S1A in pRS305 in DH5α
pVF59	pSpc19 S1D in pRS305 in DH5α
pVF60	pML10 + Spc19 WT-13xmyc in DH5α
pVF61	pML10 + Spc19 S1A-13xmyc in DH5α
pVF62	pML10 + Spc19 S1D-13xmyc in DH5α
pVF63	Spc24_S1D in pRS306 in XL10Gold
pVF64	Spc24_S2D in pRS306 in XL10Gold
pVF65	Spc24_S2A in pRS306 in XL10Gold
pVF66	pML7 + Spc19 WT-3xHA in DH5α
pVF67	pML7 + Spc19 S1A-3xHA in DH5α
pVF68	pML7 + Spc19 S1D-3xHA in DH5α
pVF69	Ipl1-WT (pRS306); no 3'UTR
pVF70	Ipl1-degron, in pPW66R

4.2 Methods

4.2.1 Yeast strain construction

Yeast strains were constructed using standard procedures:

All C-terminal tags such as S-tag-TEV-ZZ (tandem affinity purification) tag, 3xHA tags, GFP-tags and mCherry tags as well as gene deletions were integrated by PCR based approach into the yeast strain of interest (Longtine et al., 1998). ASK1 and SPC19 rescue constructs were cloned into pRS plasmids (pRS305, pRS306) as follows: Gene fragments, containing both ~ 200 bps upstream and ~ 200 bps downstream of the ORF, were generated by standard PCR on genomic DNA. These fragments were then cloned into either BamHI and XhoI sites (ASK1 in pRS306) or BamHI and ApaI (SPC19 in pRS305) of the pRS plasmids. These plasmids were then cut within the respective marker for subsequent stable integration into the genome.

Phosphorylation-site mutants were generated by using QuickChange Multi Site-Directed Mutagenesis (Agilent Technologies) on the pRS-ASK1/SPC19 plasmids. For the ASK1 gene replacement construct I cloned the full-length Ask1 without STOP codon into SmaI and SalI sites of the pML7 plasmid. ASK1-3xHA constructs including KanMX as marker were then amplified and integrated into the endogenous locus by using the Longtine strategy (Longtine et al., 1998). Growth experiments were done typically in YPD (YP + 2% dextrose), YP Raf/Gal (YP + 2% galactose and raffinose) or in minimal medium supplemented with dropout TRP and 2% dextrose.

4.2.2 Plating Assays

Yeast cells were grown overnight YPD medium containing 2% glucose. The cells were then diluted in minimal medium to an OD_{600} of 0.4. Aliquots (~5 µl) of fivefold serial dilutions of each yeast culture were spotted onto YPD plates in the absence and presence of benomyl, a microtubule depolymerizing drug (15 µg/mL). Growth differences were recorded following incubation of the plates for 48 h at 25, 30, 34 and 37°C.

4.2.3 Tandem affinity purification of Dad1-S-TEV-ZZ from yeast extracts and subsequent mass spectrometry analysis

In general the C-terminally tagged Hsk3p-S-TEV-ZZ strain was grown in YP supplemented with 2% raffinose and galactose at 30°C at 190 rpm until an $OD_{600} = 1.2$ was reached. The cultures were harvested, washed twice with ice cold PBS, resuspended in one-tenth volume of water and drop frozen in liquid nitrogen. The beads were stored at -80°C. To lyse yeast cells the frozen yeast beads were milled in a so-called freezer mill. 30 g of yeast powder were mixed with an equal volume of 2x Hyman buffer, (1x Hyman buffer: 50mM Bis-Tris Propane pH 7.0, 100mM KCl, 5mM EGTA, 5mM EDTA, 10% Glycerol, 40mM β-Glycerophosphate), 1 mM of protease inhibitors, 1 mM PMSF and 1x phosphatase inhibitor cocktail (20 mM Sodium pyrophosphate, 10 mM Sodium azide, 20 mM Sodium fluoride, 0.8 mM Sodium orthovanadate). The cell suspension was quickly thawed in a warm water bath until a homogenous suspension was obtained. From this point on the samples were kept at 4°C. Furthermore Triton X-100 to a final concentration of 1% was added. This lysate was sonicated in glass tubes for 30 seconds and afterwards centrifuged in a SS-34 rotor (Sorvall) at 15000 rpm for 25 minutes. Then the supernatant was pelleted again by ultracentrifugation in a Ti70 rotor at 45000 rpm for 30 minutes. This high-speed supernatant (HSS) was passed over a Sepharose 6 FastFlow (GE Healthcare) column (Biorad), pre-equilibrated with 1xHyman Buffer, to pre-clean the supernatant. 0.5 ml slurry of IgG Sepharose (GE Healthcare) were collected in a column and equilibrated with TST (50mM Tris-HCl pH 7.4, 150mM NaCl, 0.1% Tween20), 0.5M NH4OAc pH3.4 and finally 1xHyman buffer (300 mM KCl). Pre-equilibrated IgG sepharose was added to the HSS and 3 M KCl was added to a final concentration of 300 mM. Then the whole suspension was gently rotated at 4°C for 3 hours. After the incubation time the beads were collected in a column and washed once with 1xHyman buffer (300 mM KCl) and 1xHyman buffer (300 mM KCl + 1 mM DTT + 0.1% Tween20). The beads were resuspended in 2 mL 1xHyman buffer (300 mM KCl + 1 mM DTT + 0.1% Tween20) and incubated with 0.1 mg/mL TEV protease over night. The next day S protein agarose (Novagen) was pre-equilibrated with 1xHyman buffer. The solution of IgG sepharose beads incubated with TEV protease was passed through a column and the flow through was collected in the 2 mL Eppendorf tube together with the pre-equilibrated S protein agarose (Novagen) and again incubated for three hours by agitation at 4°C. After the incubation the beads were collected on a column and washed with 1xHyman Buffer. Proteins

were eluted with glycine by resuspending the beads gently in 60 µl 10 mM glycine pH 2.0 and further collecting the flow through in a 1,5 mL Eppendorf tube. The procedure was repeated twice. The elution showing the highest yield was subjected for subsequent MS analysis in order to identify phospho-peptides.

4.2.4 Immunoprecipitation to detect *in vivo* phosphorylation of Spc19p

Cultured cells were collected at $OD_{600} = 0.7$, washed with TBS buffer and resuspended in 700 µL lysis buffer (5% glycerol, 1 mM PMSF, complete protease inhibitor (Roche) 1:100 in TBS with or without phosphatase inhibitors: 20 mM Sodium pyrophosphate, 10 mM Sodium azide, 20 mM Sodium fluoride, 0.8 mM Sodium orthovanadate, 20 mM β-glycerophosphate,). The cells were disrupted by bead beating (Minibeadbeater, BIOSPEC) three times for 30 seconds, always putting them for two minutes on ice in between. The suspension was then incubated with additional 0.1% Tween, rotating for 30 minutes at 4°C and further pelleted by ultracentrifugation (Optima MAX XP Ultracentrifuge, Beckmann) in a TLA55 rotor at 55000 rpm for 20 minutes at 4°C. 1.5 mg of purified protein (~600 µL) were then further incubated with 30 µL of HA-coupled beads (Sigma) rotating at 4°C over night. The beads were washed three times with lysis buffer and subsequently incubated with λ-phosphatase (NEB) for 30 minutes at 30°C. The supernatant is then removed and the beads are further incubated with 50 µL of HA peptide, shaking for 30 minutes. The supernatant was then analyzed by SDS–PAGE and western blotting with monoclonal anti-HA antibodies (COVANCE).

4.2.5 Generation of Dam1 phospho-mutant expression vectors

For my *in vitro* studies I used the expression plasmid pC43HSK3H, which contains all ten Dam1 complex subunits, which are co-expressed from two different polycistronic reading frames (Miranda et al., 2005). Phosphorylation-site mutants were generated by using Phusion Site-Directed Mutagenesis (Finnzymes) on the Dam1-expression vector according to instructions provided by the manufacturer. Since mutagenesis of the ASK1/SPC19 sites in the Dam1 expression vector gave rise to a shorter product than the WT plasmid I had to cut out the mutagenized part of the smaller plasmid and religate it with the WT backbone in order to obtain the full-length vector.

4.2.6 Expression and purification of Dam1 phospho-mutants

Expression and purification of the Dam1 WT complex, the Dam1 S2D (Ask1 S216, 250D) and S3D (Ask1 S216, 250D, Spc19 S116D) complexes were performed as previously described (Westermann et al., 2005). The handling for both the Dam1 complex S2A and S3A mutants appeared somewhat more difficult. The complex was relatively unstable and showed an aggregation tendency during dialysis. Therefore I used desalting columns (GE Healthcare) with buffer B (containing 150 mM NaCl) instead of dialyzing over night.

4.2.7 Analytical gel filtration

50 μL of each Dam1 complex phospho-mutants, using approximately the same concentration for each complex (2 μM), were loaded onto the Superdex 200 PC3.2/30 (GE Healthcare). Proteins were eluted in gel filtration buffer containing 20 mM Na_2HPO_4/NaH_2PO_4, 500 mM NaCl, 1 mM EDTA, pH 6.6. Fractions of 100 μL were collected and separated by SDS-PAGE and proteins were stained with Coomassie.

4.2.8 Kinase assays

5 μL of recombinant Dam1 complex were incubated with 3 μL of Clb2-TAP tag purified Cdc28p in the Cdk1 buffer (25 mM Hepes pH 7.6, 100 mM KCl, 2 mM $MgCl_2$, 1 mM DTT, 1 mM EGTA, 5% glycerol, 20 mM β-glycerophosphate) with either 1 mM cold ATP or 5 μL γ-[^{32}P]-ATP solution (3 μL ^{32}P-ATP diluted in 110 μL kinase buffer) in a final volume of 25 μL. The reaction was performed at RT for between 0 and 60 minutes. The products from the kinase assay including γ-[^{32}P]-ATP were separated by SDS-PAGE and analyzed by autoradiography whereas the products from the cold kinase assay were subjected for subsequent MS analysis in order to detect phospho-peptides.

4.2.9 Microtubule co-sedimentation assays

The microtubule co-sedimentation assay was performed as described previously (Cheeseman et al., 2001a). 1 μM of precleared Dam1 complex was incubated with increasing concentrations of taxol-stabilized microtubules, ranging from 0 to 5 μM, that have been diluted in reaction buffer (80 mM Pipes-KOH pH 6.8, 1 mM EGTA, 1 mM $MgCl_2$, 1 mM GTP, 10 μM taxol) and additional NaCl (50, 100, 150 or 250 mM). These reactions were then incubated at RT for 20 minutes to allow binding to occur. Samples were then centrifuged for 20 minutes at 60000 rpm at 25°C (Beckmann ultracentrifuge, T100) to separate proteins bound to microtubules from not bound proteins. Proteins from pellets and supernatants were then separated by SDS-PAGE and stained by Coomassie. Intensities of bands were then quantified using MetaMorph (MDS Analytical Technologies).

4.2.10 Analysis by negative stain electron microscopy

Different concentrations of precleared Dam1 complex were incubated with 3.75 μM taxol-stabilized microtubules diluted in reaction buffer as described above. 0.5 μM were used for Dam1 WT complex and Dam1 S3D and 2 μM were used for the S3A mutant in order to see Dam1 ring formation around microtubules. The samples were then incubated at RT for 20 minutes to allow self-assembly. 3 μL of each sample are then transferred onto an electron microscopy grid carrying a carbon film that has been glow discharged. Samples were incubated for approximately 30 seconds and then carefully removed. 3 μL of 2% uranyl acetate were subsequently put onto the grid and incubated for another 30 seconds before removing the stain. Images were recorded immediately with an electron microscope operating at 80 kV (Morgagni; FEI) equipped with a CCD camera (Morada SIS; Olympus).

4.2.11 Live cell imaging

To quantify anaphase spindle dynamics, cells were arrested in G1 with α-factor, released into doTRP medium for 60 minutes before starting to record time-lapse movies. 9 z-stacks (sections 0.4 μm) were acquired at 45 seconds intervals.

To analyze Dad1-GFP signal along the metaphase spindle, cells were arrested in metaphase by using glucose as sugar source thereby repressing the Cdc20 expression from the Gal-

promoter. About 12 z-stacks (sections 0.4 μm) were acquired. Cells were plated on concanavalin A-coated coverslips. Images were recorded on a Deltavision microscope (Applied Precision, LLC) with a 100x α UPlanSApo 1.4 NA objective (Olympus) and a CCD camera (CoolSnap HQ; Photometrics) controlled by SoftWoRx software (Applied Precision, LLC) at RT. Z-stackes were deconvoluted and projected to 2D images (SoftWoRx software; Applied Precision). Images were further analyzed by MetaMorph (MDS Analytical Technologies) or ImageJ (National Institutes of Health) software.

5 References

Agarwal, R., and Cohen-Fix, O. (2002). Phosphorylation of the mitotic regulator Pds1/securin by Cdc28 is required for efficient nuclear localization of Esp1/separase. Genes Dev *16*, 1371-1382.

Alushin, G.M., Ramey, V.H., Pasqualato, S., Ball, D.A., Grigorieff, N., Musacchio, A., and Nogales, E. (2010). The Ndc80 kinetochore complex forms oligomeric arrays along microtubules. Nature *467*, 805-810.

Asbury, C.L., Gestaut, D.R., Powers, A.F., Franck, A.D., and Davis, T.N. (2006). The Dam1 kinetochore complex harnesses microtubule dynamics to produce force and movement. Proc Natl Acad Sci U S A *103*, 9873-9878.

Balasubramanian, M.K., Bi, E., and Glotzer, M. (2004). Comparative analysis of cytokinesis in budding yeast, fission yeast and animal cells. Curr Biol *14*, R806-818.

Biggins, S., and Murray, A.W. (2001). The budding yeast protein kinase Ipl1/Aurora allows the absence of tension to activate the spindle checkpoint. Genes Dev *15*, 3118-3129.

Bloom, J., and Cross, F.R. (2007). Multiple levels of cyclin specificity in cell-cycle control. Nat Rev Mol Cell Biol *8*, 149-160.

Bouck, D.C., and Bloom, K.S. (2005). The kinetochore protein Ndc10p is required for spindle stability and cytokinesis in yeast. Proc Natl Acad Sci U S A *102*, 5408-5413.

Chee, M.K., and Haase, S.B. (2010). B-cyclin/CDKs regulate mitotic spindle assembly by phosphorylating kinesins-5 in budding yeast. PLoS Genet *6*, e1000935.

Cheeseman, I.M., Anderson, S., Jwa, M., Green, E.M., Kang, J., Yates, J.R., 3rd, Chan, C.S., Drubin, D.G., and Barnes, G. (2002). Phospho-regulation of kinetochore-microtubule attachments by the Aurora kinase Ipl1p. Cell *111*, 163-172.

Cheeseman, I.M., Brew, C., Wolyniak, M., Desai, A., Anderson, S., Muster, N., Yates, J.R., Huffaker, T.C., Drubin, D.G., and Barnes, G. (2001a). Implication of a novel multiprotein Dam1p complex in outer kinetochore function. J Cell Biol *155*, 1137-1145.

Cheeseman, I.M., Chappie, J.S., Wilson-Kubalek, E.M., and Desai, A. (2006). The conserved KMN network constitutes the core microtubule-binding site of the kinetochore. Cell *127*, 983-997.

Cheeseman, I.M., Enquist-Newman, M., Muller-Reichert, T., Drubin, D.G., and Barnes, G. (2001b). Mitotic spindle integrity and kinetochore function linked by the Duo1p/Dam1p complex. J Cell Biol *152*, 197-212.

Cheeseman, I.M., Niessen, S., Anderson, S., Hyndman, F., Yates, J.R., 3rd, Oegema, K., and Desai, A. (2004). A conserved protein network controls assembly of the outer kinetochore and its ability to sustain tension. Genes Dev *18*, 2255-2268.

De Wulf, P., McAinsh, A.D., and Sorger, P.K. (2003). Hierarchical assembly of the budding yeast kinetochore from multiple subcomplexes. Genes Dev *17*, 2902-2921.

Dirick, L., Bohm, T., and Nasmyth, K. (1995). Roles and regulation of Cln-Cdc28 kinases at the start of the cell cycle of Saccharomyces cerevisiae. EMBO J *14*, 4803-4813.

Enquist-Newman, M., Cheeseman, I.M., Van Goor, D., Drubin, D.G., Meluh, P.B., and Barnes, G. (2001). Dad1p, third component of the Duo1p/Dam1p complex involved in kinetochore function and mitotic spindle integrity. Mol Biol Cell *12*, 2601-2613.

Enserink, J.M., and Kolodner, R.D. (2010). An overview of Cdk1-controlled targets and processes. Cell Div *5*, 11.

Espelin, C.W., Kaplan, K.B., and Sorger, P.K. (1997). Probing the architecture of a simple kinetochore using DNA-protein crosslinking. J Cell Biol *139*, 1383-1396.

Euskirchen, G.M. (2002). Nnf1p, Dsn1p, Mtw1p, and Nsl1p: a new group of proteins important for chromosome segregation in Saccharomyces cerevisiae. Eukaryot Cell *1*, 229-240.

Fitzgerald-Hayes, M., Clarke, L., and Carbon, J. (1982). Nucleotide sequence comparisons and functional analysis of yeast centromere DNAs. Cell *29*, 235-244.

Gerson-Gurwitz, A., Movshovich, N., Avunie, R., Fridman, V., Moyal, K., Katz, B., Hoyt, M.A., and Gheber, L. (2009). Mid-anaphase arrest in S. cerevisiae cells eliminated for the function of Cin8 and dynein. Cell Mol Life Sci *66*, 301-313.

Gestaut, D.R., Graczyk, B., Cooper, J., Widlund, P.O., Zelter, A., Wordeman, L., Asbury, C.L., and Davis, T.N. (2008). Phosphoregulation and depolymerization-driven movement of the Dam1 complex do not require ring formation. Nat Cell Biol.

Gheber, L., Kuo, S.C., and Hoyt, M.A. (1999). Motile properties of the kinesin-related Cin8p spindle motor extracted from Saccharomyces cerevisiae cells. J Biol Chem *274*, 9564-9572.

Ghosh, S.K., Poddar, A., Hajra, S., Sanyal, K., and Sinha, P. (2001). The IML3/MCM19 gene of Saccharomyces cerevisiae is required for a kinetochore-related process during chromosome segregation. Mol Genet Genomics *265*, 249-257.

Goshima, G., and Yanagida, M. (2000). Establishing biorientation occurs with precocious separation of the sister kinetochores, but not the arms, in the early spindle of budding yeast. Cell *100*, 619-633.

Grishchuk, E.L., Spiridonov, I.S., Volkov, V.A., Efremov, A., Westermann, S., Drubin, D., Barnes, G., Ataullakhanov, F.I., and McIntosh, J.R. (2008). Different assemblies of the DAM1 complex follow shortening microtubules by distinct mechanisms. Proc Natl Acad Sci U S A *105*, 6918-6923.

He, X., Rines, D.R., Espelin, C.W., and Sorger, P.K. (2001). Molecular analysis of kinetochore-microtubule attachment in budding yeast. Cell *106*, 195-206.

Hegemann, J.H., and Fleig, U.N. (1993). The centromere of budding yeast. Bioessays *15*, 451-460.

Higuchi, T., and Uhlmann, F. (2005). Stabilization of microtubule dynamics at anaphase onset promotes chromosome segregation. Nature *433*, 171-176.

Hofmann, C., Cheeseman, I.M., Goode, B.L., McDonald, K.L., Barnes, G., and Drubin, D.G. (1998). Saccharomyces cerevisiae Duo1p and Dam1p, novel proteins involved in mitotic spindle function. J Cell Biol *143*, 1029-1040.

Holt, L.J., Tuch, B.B., Villen, J., Johnson, A.D., Gygi, S.P., and Morgan, D.O. (2009). Global analysis of Cdk1 substrate phosphorylation sites provides insights into evolution. Science *325*, 1682-1686.

Hornung, P., Maier, M., Alushin, G.M., Lander, G.C., Nogales, E., and Westermann, S. (2010). Molecular Architecture and Connectivity of the Budding Yeast Mtw1 Kinetochore Complex. J Mol Biol.

Huang, B., and Huffaker, T.C. (2006). Dynamic microtubules are essential for efficient chromosome capture and biorientation in S. cerevisiae. J Cell Biol *175*, 17-23.

Ikeuchi, A., Nakano, H., Kamiya, T., Yamane, T., and Kawarasaki, Y. (2010). A method for reverse interactome analysis: High-resolution mapping of interdomain interaction network in Dam1 complex and its specific disorganization based on the interaction domain expression. Biotechnol Prog *26*, 945-953.

Ito, T., Chiba, T., Ozawa, R., Yoshida, M., Hattori, M., and Sakaki, Y. (2001). A comprehensive two-hybrid analysis to explore the yeast protein interactome. Proc Natl Acad Sci U S A *98*, 4569-4574.

Janke, C., Ortiz, J., Lechner, J., Shevchenko, A., Shevchenko, A., Magiera, M.M., Schramm, C., and Schiebel, E. (2001). The budding yeast proteins Spc24p and Spc25p interact with Ndc80p and Nuf2p at the kinetochore and are important for kinetochore clustering and checkpoint control. Embo J *20*, 777-791.

Janke, C., Ortiz, J., Tanaka, T.U., Lechner, J., and Schiebel, E. (2002). Four new subunits of the Dam1-Duo1 complex reveal novel functions in sister kinetochore biorientation. Embo J *21*, 181-193.

Jaspersen, S.L., Charles, J.F., and Morgan, D.O. (1999). Inhibitory phosphorylation of the APC regulator Hct1 is controlled by the kinase Cdc28 and the phosphatase Cdc14. Curr Biol *9*, 227-236.

Jaspersen, S.L., Huneycutt, B.J., Giddings, T.H., Jr., Resing, K.A., Ahn, N.G., and Winey, M. (2004). Cdc28/Cdk1 regulates spindle pole body duplication through phosphorylation of Spc42 and Mps1. Dev Cell *7*, 263-274.

Jaspersen, S.L., and Winey, M. (2004). The budding yeast spindle pole body: structure, duplication, and function. Annu Rev Cell Dev Biol *20*, 1-28.

Jensen, S., Segal, M., Clarke, D.J., and Reed, S.I. (2001). A novel role of the budding yeast separin Esp1 in anaphase spindle elongation: evidence that proper spindle association of Esp1 is regulated by Pds1. J Cell Biol *152*, 27-40.

Joglekar, A.P., Bouck, D.C., Molk, J.N., Bloom, K.S., and Salmon, E.D. (2006). Molecular architecture of a kinetochore-microtubule attachment site. Nat Cell Biol *8*, 581-585.

Jones, M.H., Bachant, J.B., Castillo, A.R., Giddings, T.H., Jr., and Winey, M. (1999). Yeast Dam1p is required to maintain spindle integrity during mitosis and interacts with the Mps1p kinase. Mol Biol Cell *10*, 2377-2391.

Jones, M.H., He, X., Giddings, T.H., and Winey, M. (2001). Yeast Dam1p has a role at the kinetochore in assembly of the mitotic spindle. Proc Natl Acad Sci U S A *98*, 13675-13680.

Keith, K.C., and Fitzgerald-Hayes, M. (2000). CSE4 genetically interacts with the Saccharomyces cerevisiae centromere DNA elements CDE I and CDE II but not CDE III. Implications for the path of the centromere dna around a cse4p variant nucleosome. Genetics *156*, 973-981.

Khmelinskii, A., Roostalu, J., Roque, H., Antony, C., and Schiebel, E. (2009). Phosphorylation-dependent protein interactions at the spindle midzone mediate cell cycle regulation of spindle elongation. Dev Cell *17*, 244-256.

Kirschner, M., and Mitchison, T. (1986). Beyond self-assembly: from microtubules to morphogenesis. Cell *45*, 329-342.

Kline-Smith, S.L., and Walczak, C.E. (2004). Mitotic spindle assembly and chromosome segregation: refocusing on microtubule dynamics. Mol Cell *15*, 317-327.

Kotani, S., Tanaka, H., Yasuda, H., and Todokoro, K. (1999). Regulation of APC activity by phosphorylation and regulatory factors. J Cell Biol *146*, 791-800.

Kramer, E.R., Scheuringer, N., Podtelejnikov, A.V., Mann, M., and Peters, J.M. (2000). Mitotic regulation of the APC activator proteins CDC20 and CDH1. Mol Biol Cell *11*, 1555-1569.

Lampert, F., Hornung, P., and Westermann, S. (2010). The Dam1 complex confers microtubule plus end-tracking activity to the Ndc80 kinetochore complex. J Cell Biol *189*, 641-649.

Lampert, F., and Westermann, S. (2011). A blueprint for kinetochores - new insights into the molecular mechanics of cell division. Nat Rev Mol Cell Biol *12*, 407-412.

Lampson, M.A., and Cheeseman, I.M. (2010). Sensing centromere tension: Aurora B and the regulation of kinetochore function. Trends Cell Biol.

Lechner, J., and Carbon, J. (1991). A 240 kd multisubunit protein complex, CBF3, is a major component of the budding yeast centromere. Cell *64*, 717-725.

Li, Y., Bachant, J., Alcasabas, A.A., Wang, Y., Qin, J., and Elledge, S.J. (2002). The mitotic spindle is required for loading of the DASH complex onto the kinetochore. Genes Dev *16*, 183-197.

Li, Y., and Elledge, S.J. (2003). The DASH complex component Ask1 is a cell cycle-regulated Cdk substrate in Saccharomyces cerevisiae. Cell Cycle *2*, 143-148.

Liakopoulos, D., Kusch, J., Grava, S., Vogel, J., and Barral, Y. (2003). Asymmetric loading of Kar9 onto spindle poles and microtubules ensures proper spindle alignment. Cell *112*, 561-574.

Longtine, M.S., McKenzie, A., 3rd, Demarini, D.J., Shah, N.G., Wach, A., Brachat, A., Philippsen, P., and Pringle, J.R. (1998). Additional modules for versatile and economical PCR-based gene deletion and modification in Saccharomyces cerevisiae. Yeast *14*, 953-961.

Maddox, P.S., Bloom, K.S., and Salmon, E.D. (2000). The polarity and dynamics of microtubule assembly in the budding yeast Saccharomyces cerevisiae. Nat Cell Biol *2*, 36-41.

Mallavarapu, A., Sawin, K., and Mitchison, T. (1999). A switch in microtubule dynamics at the onset of anaphase B in the mitotic spindle of Schizosaccharomyces pombe. Curr Biol *9*, 1423-1426.

McAinsh, A.D., Tytell, J.D., and Sorger, P.K. (2003). Structure, function, and regulation of budding yeast kinetochores. Annu Rev Cell Dev Biol *19*, 519-539.

Meluh, P.B., and Koshland, D. (1995). Evidence that the MIF2 gene of Saccharomyces cerevisiae encodes a centromere protein with homology to the mammalian centromere protein CENP-C. Mol Biol Cell *6*, 793-807.

Meluh, P.B., Yang, P., Glowczewski, L., Koshland, D., and Smith, M.M. (1998). Cse4p is a component of the core centromere of Saccharomyces cerevisiae. Cell *94*, 607-613.

Mendenhall, M.D., and Hodge, A.E. (1998). Regulation of Cdc28 cyclin-dependent protein kinase activity during the cell cycle of the yeast Saccharomyces cerevisiae. Microbiol Mol Biol Rev *62*, 1191-1243.

Mimura, S., Seki, T., Tanaka, S., and Diffley, J.F. (2004). Phosphorylation-dependent binding of mitotic cyclins to Cdc6 contributes to DNA replication control. Nature *431*, 1118-1123.

Miranda, J.J., De Wulf, P., Sorger, P.K., and Harrison, S.C. (2005). The yeast DASH complex forms closed rings on microtubules. Nat Struct Mol Biol *12*, 138-143.

Morgan, D.O. (1997). Cyclin-dependent kinases: engines, clocks, and microprocessors. Annu Rev Cell Dev Biol *13*, 261-291.

Morgan, D.O. (2006). The cell cycle : principles of control (London, New Science Press ; Oxford : Oxford University Press [distributor]).

Morgan, D.O. (2007). The Cell Cycle - Principles of Control. New Science Press.

Movshovich, N., Fridman, V., Gerson-Gurwitz, A., Shumacher, I., Gertsberg, I., Fich, A., Hoyt, M.A., Katz, B., and Gheber, L. (2008). Slk19-dependent mid-anaphase pause in kinesin-5-mutated cells. J Cell Sci *121*, 2529-2539.

Murray, A., and Hunt, T. (1993). The Cell Cycle - an introduction. Oxford University Press.

Nakajima, Y., Cormier, A., Tyers, R.G., Pigula, A., Peng, Y., Drubin, D.G., and Barnes, G. (2011). Ipl1/Aurora-dependent phosphorylation of Sli15/INCENP regulates CPC-spindle interaction to ensure proper microtubule dynamics. J Cell Biol *194*, 137-153.

Nekrasov, V.S., Smith, M.A., Peak-Chew, S., and Kilmartin, J.V. (2003). Interactions between centromere complexes in Saccharomyces cerevisiae. Mol Biol Cell *14*, 4931-4946.

Oliveira, R.A., Hamilton, R.S., Pauli, A., Davis, I., and Nasmyth, K. (2010). Cohesin cleavage and Cdk inhibition trigger formation of daughter nuclei. Nat Cell Biol *12*, 185-192.

Pagliuca, C., Draviam, V.M., Marco, E., Sorger, P.K., and De Wulf, P. (2009). Roles for the conserved spc105p/kre28p complex in kinetochore-microtubule binding and the spindle assembly checkpoint. PLoS One *4*, e7640.

Pereira, G., and Schiebel, E. (2003). Separase regulates INCENP-Aurora B anaphase spindle function through Cdc14. Science *302*, 2120-2124.

Peters, J.M. (2006). The anaphase promoting complex/cyclosome: a machine designed to destroy. Nat Rev Mol Cell Biol *7*, 644-656.

Peters, J.M., Tedeschi, A., and Schmitz, J. (2008). The cohesin complex and its roles in chromosome biology. Genes Dev *22*, 3089-3114.

Pinsky, B.A., Kung, C., Shokat, K.M., and Biggins, S. (2006). The Ipl1-Aurora protein kinase activates the spindle checkpoint by creating unattached kinetochores. Nat Cell Biol *8*, 78-83.

Queralt, E., and Uhlmann, F. (2008). Cdk-counteracting phosphatases unlock mitotic exit. Curr Opin Cell Biol *20*, 661-668.

Ramey, V.H., Wong, A., Fang, J., Howes, S., Barnes, G., and Nogales, E. (2011). Subunit organization in the Dam1 kinetochore complex and its ring around microtubules. Mol Biol Cell.

Richardson, H., Lew, D.J., Henze, M., Sugimoto, K., and Reed, S.I. (1992). Cyclin-B homologs in Saccharomyces cerevisiae function in S phase and in G2. Genes Dev *6*, 2021-2034.

Santaguida, S., and Musacchio, A. (2009). The life and miracles of kinetochores. Embo J *28*, 2511-2531.

Saunders, W.S., Koshland, D., Eshel, D., Gibbons, I.R., and Hoyt, M.A. (1995). Saccharomyces cerevisiae kinesin- and dynein-related proteins required for anaphase chromosome segregation. J Cell Biol *128*, 617-624.

Schwob, E., and Nasmyth, K. (1993). CLB5 and CLB6, a new pair of B cyclins involved in DNA replication in Saccharomyces cerevisiae. Genes Dev *7*, 1160-1175.

Shang, C., Hazbun, T.R., Cheeseman, I.M., Aranda, J., Fields, S., Drubin, D.G., and Barnes, G. (2003). Kinetochore protein interactions and their regulation by the Aurora kinase Ipl1p. Mol Biol Cell *14*, 3342-3355.

Shimogawa, M.M., Graczyk, B., Gardner, M.K., Francis, S.E., White, E.A., Ess, M., Molk, J.N., Ruse, C., Niessen, S., Yates, J.R., 3rd*, et al.* (2006). Mps1 phosphorylation of Dam1 couples kinetochores to microtubule plus ends at metaphase. Curr Biol *16*, 1489-1501.

Straight, A.F., Marshall, W.F., Sedat, J.W., and Murray, A.W. (1997). Mitosis in living budding yeast: anaphase A but no metaphase plate. Science (New York, NY *277*, 574-578.

Straight, A.F., Sedat, J.W., and Murray, A.W. (1998). Time-lapse microscopy reveals unique roles for kinesins during anaphase in budding yeast. J Cell Biol *143*, 687-694.

Stuart, D., and Wittenberg, C. (1995). CLN3, not positive feedback, determines the timing of CLN2 transcription in cycling cells. Genes Dev *9*, 2780-2794.

Tanaka, T.U., Rachidi, N., Janke, C., Pereira, G., Galova, M., Schiebel, E., Stark, M.J., and Nasmyth, K. (2002). Evidence that the Ipl1-Sli15 (Aurora kinase-INCENP) complex promotes chromosome bi-orientation by altering kinetochore-spindle pole connections. Cell *108*, 317-329.

Tanaka, T.U., Stark, M.J., and Tanaka, K. (2005). Kinetochore capture and bi-orientation on the mitotic spindle. Nat Rev Mol Cell Biol *6*, 929-942.

Thornton, B.R., Ng, T.M., Matyskiela, M.E., Carroll, C.W., Morgan, D.O., and Toczyski, D.P. (2006). An architectural map of the anaphase-promoting complex. Genes Dev *20*, 449-460.

Tien, J.F., Umbreit, N.T., Gestaut, D.R., Franck, A.D., Cooper, J., Wordeman, L., Gonen, T., Asbury, C.L., and Davis, T.N. (2010). Cooperation of the Dam1 and Ndc80 kinetochore complexes enhances microtubule coupling and is regulated by aurora B. J Cell Biol *189*, 713-723.

Tyers, M., Tokiwa, G., and Futcher, B. (1993). Comparison of the Saccharomyces cerevisiae G1 cyclins: Cln3 may be an upstream activator of Cln1, Cln2 and other cyclins. EMBO J *12*, 1955-1968.

Ubersax, J.A., Woodbury, E.L., Quang, P.N., Paraz, M., Blethrow, J.D., Shah, K., Shokat, K.M., and Morgan, D.O. (2003). Targets of the cyclin-dependent kinase Cdk1. Nature *425*, 859-864.

Wang, H.W., Ramey, V.H., Westermann, S., Leschziner, A.E., Welburn, J.P., Nakajima, Y., Drubin, D.G., Barnes, G., and Nogales, E. (2007). Architecture of the Dam1 kinetochore ring complex and implications for microtubule-driven assembly and force-coupling mechanisms. Nat Struct Mol Biol *14*, 721-726.

Wei, R.R., Al-Bassam, J., and Harrison, S.C. (2007). The Ndc80/HEC1 complex is a contact point for kinetochore-microtubule attachment. Nat Struct Mol Biol *14*, 54-59.

Westermann, S., Avila-Sakar, A., Wang, H.W., Niederstrasser, H., Wong, J., Drubin, D.G., Nogales, E., and Barnes, G. (2005). Formation of a dynamic kinetochore- microtubule interface through assembly of the Dam1 ring complex. Mol Cell *17*, 277-290.

Westermann, S., Drubin, D.G., and Barnes, G. (2007). Structures and functions of yeast kinetochore complexes. Annu Rev Biochem *76*, 563-591.

Westermann, S., Wang, H.W., Avila-Sakar, A., Drubin, D.G., Nogales, E., and Barnes, G. (2006). The Dam1 kinetochore ring complex moves processively on depolymerizing microtubule ends. Nature *440*, 565-569.

Widlund, P.O., Lyssand, J.S., Anderson, S., Niessen, S., Yates, J.R., 3rd, and Davis, T.N. (2006). Phosphorylation of the chromosomal passenger protein Bir1 is required for localization of Ndc10 to the spindle during anaphase and full spindle elongation. Mol Biol Cell *17*, 1065-1074.

Wigge, P.A., and Kilmartin, J.V. (2001). The Ndc80p complex from Saccharomyces cerevisiae contains conserved centromere components and has a function in chromosome segregation. J Cell Biol *152*, 349-360.

Wong, J., Nakajima, Y., Westermann, S., Shang, C., Kang, J.S., Goodner, C., Houshmand, P., Fields, S., Chan, C.S., Drubin, D.*, et al.* (2007). A protein interaction map of the mitotic spindle. Mol Biol Cell *18*, 3800-3809.

Woodbury, E.L., and Morgan, D.O. (2007). Cdk and APC activities limit the spindle-stabilizing function of Fin1 to anaphase. Nat Cell Biol *9*, 106-112.

Yoon, H.J., Feoktistova, A., Wolfe, B.A., Jennings, J.L., Link, A.J., and Gould, K.L. (2002). Proteomics analysis identifies new components of the fission and budding yeast anaphase-promoting complexes. Curr Biol *12*, 2048-2054.

Zachariae, W., Schwab, M., Nasmyth, K., and Seufert, W. (1998a). Control of cyclin ubiquitination by CDK-regulated binding of Hct1 to the anaphase promoting complex. Science *282*, 1721-1724.

Zachariae, W., Shevchenko, A., Andrews, P.D., Ciosk, R., Galova, M., Stark, M.J., Mann, M., and Nasmyth, K. (1998b). Mass spectrometric analysis of the anaphase-promoting complex from yeast: identification of a subunit related to cullins. Science *279*, 1216-1219.

Zhai, Y., Kronebusch, P.J., and Borisy, G.G. (1995). Kinetochore microtubule dynamics and the metaphase-anaphase transition. J Cell Biol *131*, 721-734.

Zinkowski, R.P., Meyne, J., and Brinkley, B.R. (1991). The centromere-kinetochore complex: a repeat subunit model. J Cell Biol *113*, 1091-1110.

6 Acknowledgement

7 Curriculum Vitae

Personal information:

Name: Veronika Fitz

Nationality: Austrian

Date of Birth: 22nd July 1983 in Feldkirch, Austria

Email: veronika.fitz@imp.ac.at

Education:

2005 – present	Studies of Molecular Biology
	University of Vienna, Austria
06 – 09/2010	LRI Summer School
	Cancer Research UK, London Research Institute
2002 – 2004	Studies of Medicine
	University of Vienna/University of Medicine, Austria
2002 – 2003	Studies of French
	University of Vienna, Austria
2001 – 2002	Studies of French
	University of Perpignan, France
1993 – 2001	Bundesgymnasium Dornbirn, Austria
	Graduation with distinction